HAWASSA UNIVERSITY
INSTITUTE OF TECHNOLOGY
FACULTY OF ELECTRICAL ENGINEERING
DEPARTMENT OF ELECTRICAL AND COMPUTER ENGINEERING

PERFORMANCE ANALYSIS OF HYBRID OPTICAL FIBER/FSO COMMUNICATION SYSTEM USING ADVANCED MODULATIONS

BY
FISEHA ZELALEM
ADVISOR: DR. MERHAWIT BERHANE (Ph.D.)
CO-ADVISOR: ALEMAYEHU CHERU (M.Sc.)

A THESIS
SUBMITTED TO THE DEPARTMENT OF ELECTRICAL AND COMPUTER ENGINEERING IN PARTIAL FULFILLMENT OF THE REQUIREMENTS
FOR THE DEGREE OF
MASTER OF SCIENCE
IN
COMMUNICATION ENGINEERING AND NETWORKING

HAWASSA, ETHIOPIA
SEPTEMBER, 2021

HAWASSA UNIVERSITY

SCHOOL OF GRADUATE STUDIES

EXAMINERS' APPROVAL SHEET

As members of the board of examiners of the final master's degree open defense. we certify that we have lead evaluated the thesis prepared by Fiseha Zelalem under the title Performance Analysis of Hybrid Optical Fiber/FSO Communication System Using Advanced Modulations and recommend that it be accepted as fulfilling the thesis requirement for the degree of M.Sc. in Communication Engineering and Networking.

Name of chairperson	signature	date
(M.Sc.)		
Name of internal examiner	signature	date
Zelalem Hailu (Ph.D.)		04/11/2021
Name of external examiner	signature	date
Dr. Merhawit Berhane (Ph.D.)		
Name of principal advisor	signature	date
Alemayehu Cheru (M.Sc.)		
Name of Co-advisor	signature	date

Final approval and acceptance of the contingent upon the submission of the final copy of the thesis to the SG and DGC/SGC of the candidate department

Thesis approved by

SGS	signature	date

Declaration

I hereby declare that this M.Sc. thesis is my original work and has not been presented for a degree in Hawassa University and other institutions, and all sources of material used for this thesis have been duly acknowledged.

Fiseha Zelalem	----------	----------
Name of student	Signature	Date

This M.Sc. thesis has been submitted for examination with my approval as a thesis advisor.

Dr. Merhawit Berhane (Ph.D.)	_____	_____
Name of Advisor	signature	date

Alemayehu Cheru (M.Sc.)	_____	_____
Name of Co-Advisor	signature	date

September, 2021

Abstract

Due to its lower attenuation and high bandwidth, current telecommunication infrastructure uses optical fibers for high data long haul transmission. Free space optics (FSO) technology is a good option for short-distance multi-gigabits per second or beyond data transmission. Nowadays, it has different application areas such as indoor, outdoor, underwater, and deep-space communications. A key area within this new generation is the combination of optical fiber and FSO network to provide high bandwidth for both long and short-distance services.

The hybrid link uses coherent optical advanced modulation and dispersion compensation techniques to achieve the best performance with the existence of atmospheric turbulence effect and fiber limitations. Orthogonal frequency division multiplexing (OFDM) and dual-polarization quadrature phase-shift keying (DP-QPSK) are considered promising technologies to satisfy the demand for bandwidth expansion in broadband services. OFDM can overwhelm optical fiber limitations such as polarization mode dispersion (PMD) and chromatic dispersion (CD), whereas DP-QPSK provides good noise immunity.

This thesis concentrates on designing, simulation, and performance analysis of 100Gbits/s data rate hybrid optical fiber/FSO systems using coherent optical OFDM and DP-QPSK modulation techniques. MATLAB software and OptiSystem simulation tool are used to design and simulate the hybrid system. To study the performance of the systems and the quality of the signals the bit error rate and the Q-factor are considered. As a result, for 100Gbits/s per channel with DP-QPSK based system, the link coverage is up to 468m in FSO and 202km by fiber cable; and up to 510m FSO link and 220km by fiber optics for CO-OFDM system. It is observed that the CO-OFDM system has high tolerance against linear signal distortion effects and sensitive to nonlinear effects which affects the system performance.

Keywords: Hybrid fiber/FSO, FSO, DP-QPSK, OFDM, Coherent Optical.

Acknowledgments

First of all, I would like to thank GOD, for blessing me that this thesis can be done successfully. I would like to express our deep and sincere gratitude to my advisor Dr. Merhawit Berhane (Ph.D.) for her instructions, contentious encouragement, valuable discussion and support throughout the whole process of this thesis. In addition, I am great thanks to my co-advisor Alemayehu Cheru (M.Sc.) for his valuable discussion and support throughout the thesis work. A special thanks to the Electrical and Computer Engineering department for providing me adequate computer laboratory infrastructure to carry out this thesis.

Lastly, I offer my regards and blessings to all of those who supported me in any respect during the completion of the thesis, particularly my dearest family and all my friends for their sincere supplication, feelings, and love throughout the whole master study and the work with this thesis.

Table of Contents

List of Tables

List of Figures

List of Abbreviations

Acronym	Description
4G	Fourth Generation
5G	Fifth Generation
ADC	Analog to Digital convertor
AWGN	Additive White Gaussian Noise
BW	Bandwidth
CAP	Carrier-less Amplitude Modulation
CD	Chromatic Dispersion
CMOS	Complementary Metal Oxide Semiconductor
CO-OFDM	Coherent Optical-Orthogonal Frequency Division Multiplexing
CW	Continues Wave
DAC	Digital to Analog Convertor
DCN	Data Center Network
DLI	Delay-Line Interferometer
DMT	Discrete Multi-Tone
DPC	Dynamic Polarization alignment Controller
DP-QPSK	Dual polarization Quadrature Phase Shift-Keying
DSL	Digital Subscriber Line
EMI	Electro-Magnetic Interference
FFT	Fast Fourier Transform
FDM	Frequency Division Multiplexing
FSO	Free Space Optical
Gbps/Gbits/s	Giga bit per second

GHz	Giga Hertz
GVD	Group Velocity Dispersion
ICI	Inter Carrier Interference
IFFT	Inverse Fast Fourier Transform
IM-DD	Intensity Modulation-Direct Detection
IoT	Internet of Things
ISI	Inter Symbol Interference
I/Q	In-phase/Quadrature
LAN	Local Area Network
LED	Light Emitting Diode
LD	Laser Diode
LPF	Low Pass Filter
MAN	Metropolitan Area Network
M-PSK	M-phase shift Keying
mm-Wave	millimeter Wave
OSNR	Optical Signal to Noise Ratio
PAPR	Peak to Average Power Ratio
PBS	Polarization beam Splitter
PMD	Polarization Mode Dispersion
PPM	Pulse Position Modulation
PSK	Phase Shift Keying
Q-factor	Quality factor
QAM	Quadrature Amplitude Modulation
DCN	Data Center Network
RF	Radio Frequency
Tbps	Terra bits per second
UDWDM	Ultra Dense Wavelength Division Multiplexing
UOWC	Underwater Optical Wireless Communication

Notations

Notation	Description
exp[.]	Exponent
A	Input base band signal amplitude
A_{eff}	Effective fiber area
B	Signal amplitude at PD input
c	Speed of light
CMA	Constant modulus algorithm
CPE	Carrier Phase Estimation
D	Dispersion
DBP	Digital backward propagation
DSP	Digital signal processing
f_c	Optical carrier frequency
FOE	Frequency Offset Estimation
$E_{i,PD}$	The input electrical field of photo detector
E_{LD}	Electrical field of the laser diode
E_{MZo}	Output electrical field of the MZM
G	Optical amplifier gain
i_{PD}	Photocurrent of photo detector
exr	Extinction ratio

L	Length of fiber
l	Length of MZM electrode
n	Refractive index
n_2	Nonlinear refractive index
P_{INo}	The average input power of laser diode
T_s	Symbol period
$v_{1,2}$	The drive voltages of the MZM
v_π	Half wave voltage of the MZM
v_g	The group velocity
z	Amplifier space distance
α	Attenuation
β	Modulation coefficient of the MZM
β_2	Group velocity dispersion
ε_0	Dielectric constant of air
λ	Wave length
θ_i	The i^{th}phase angle
ϑ	Nonlinear coefficient
φ	The phase angle of the LD field
$\varphi_{I,Q,PSK}$	PSK base band signal

$\emptyset_{NL}$	Nonlinear phase shift
$\Gamma(.)$	Gamma function
γ	Power splitting ratio of the Y-junction
א	The wave propagation coefficient

Presentation comments

No.	Comments	Remarks
1	Abstract needs to be improved since there is redundancy of words and unclear sentence.	Revised
2	Use of inappropriate terms in the general objective.	Revised
3	Use of inappropriate words and improvement of specific objectives.	Revised
4	Specify the scope of the thesis.	Revised
5	Organization of the thesis for chapter 2-4.	Merged in to 2 chapters
6	Is your system single channel or WDM based?	Single channel
7	Fiber length specification in the sample simulation 50 or 100Km?	50km
8	Doubts in simulation parameters (global and SMF parameters).	Revised
9	Doubts on the optical ASE noise bandwidth.	Standard SMF with 1550nm is considered and the ASE noise BW is approximated 0.1nm.
10	The explanation of simulation result on Q-factor vs BER.	Revised
11	Simulation result doubts on nonlinear and linear dispersion effects.	Revised
12	Effect of dispersion, FWM, SPM, and XPM for each scheme and also BER calculation.	Revised
13	Addition of unnecessary results in conclusion part.	Revised
14	Citation of figures.	

CHAPTER ONE

Introduction

1.1 Overview

The increase in network traffic has forced telecommunication technologies to focus on the expansion of communication bandwidth for high data rate transmission. Along with enhancing the bandwidth of the communication link efficient performance should take great attention to meet the new generation requirements. Employment of high optical bands will relieve the problems due to spectrum deficiency in radio frequency (RF) based communication systems. Optical free-space communication systems are cost-effective and energy-efficient for high-speed and highly secure wireless connections while optical fiber has advantages of transmitting data over long distances with greater information-carrying capacity, less attenuation, and electromagnetic interference (EMI) [3-5 and 9]. But optical fiber technologies induce dispersion and non-linearity effects which require compensation techniques. In another way, free-space optics is a line of sight communication technique suited for last and first-mile data transmission in both indoor and outdoor areas [6, 7]. It is more advantageous due to its unregulated spectrum, and low deployment cost. Thus, the integration of an optical fiber with a free-space link can form a hybrid optical fiber/FSO communication system that can handle higher data rates for long and short-distance transmissions [1, 2, and 9].

Recently, researchers are being shown to come across the high capacity demand in the communication systems, primarily for multi-Gbits/s and Tbits/s. First and last-mile access networks are currently well-thought-out as encouraging ways for both service providers and end-users in terms of minimizing deployment cost and upgrading period, improving mobility, and enhancing the flexibility of broadband services. The two key concerns that need to be known to increases the transmission rate per channel are the expansion of bandwidth and improving spectral efficiency.

1.1.1 System bandwidth expansion

Increasing the transmission bandwidth per channel either optically or electronically is one of the methods to enhance the capacity of a transmitting system. In optical transmission networks, there are two commonly used ways to improve the capacity of the transmission system [4, 8]. The first one is by tallying several optical carriers which have already been considered and deployed and are known as wavelength division multiplexing (WDM). It is well-thought-out one of the most cost-efficient methods to increase the optical fiber link throughput [2, 11]. The second method is to expand the component bandwidth per channel using semiconductor technology.

1.1.2 Enhancing the spectral efficiency

In optical network systems, the most important figure of merit is spectral efficiency which is the carrying capacity of information per unit bandwidth. Currently, many optical networks use intensity modulation with direct detection for high data transmission. However, the spectral efficiency with binary modulation will not exceed 1 bits/s/Hz; multiple advanced modulation techniques have been explored to improve the capacity of the transmission systems. Combining coherent detection with advanced modulation techniques can easily achieve the spectral efficiency of several bits/s/Hz per channel [10]. Some of these formats are the coherent optical OFDM and DP-QPSK.

Orthogonal frequency division multiplexing (OFDM) is a frequency division multiplexing (FDM) scheme used for coding digital data on different carrier frequencies. It has two vital benefits which are robustness against channel dispersion and ease of phase and channel estimation in a time-fluctuating environment. Several sub-carriers are oriented closely spaced to convey data on multiple channels [8]. It uses QAM or PSK modulation scheme to modulate each sub-carrier.

A cost-effective system can be designed through the reduction of the network modules that require a lower number of wavelengths. Thus, applying a multilevel modulation technique can be a potential choice to reduce the complexity and costs of optoelectronic components as well further improve spectral efficiency. Therefore, an optical network system will be more realistic and effective if the employment of advanced modulation techniques can reduce the complexity of the system while simultaneously enhance spectral efficiency.

Dual polarization quadrature phase-shift keying (DP QPSK) is an extension of the ordinary quadrature phase-shift keying **(**QPSK) modulation which consists of two orthogonal states of polarization (horizontal and vertical) of light intensity. It uses I/Q QPSK modulators signal to encode 4 bits/symbol rate at a time and is advantageous in decreasing the BW of the transmission of information. In the DP-QPSK scheme, the system data is encoded in both phase and polarization.

1.2 Statement of the Problem

The current radio frequency system cannot satisfy the growth in demand of telecommunication network systems to transmit high data rate with efficient performance. The two key concerns that need to be known to increases the transmission rate per channel are the expansion of bandwidth and improving spectral efficiency.

First and last-mile access networks are currently well-thought-out as encouraging ways for both service providers and end-users in terms of minimizing deployment cost and upgrading period, improving mobility, and enhancing the flexibility of broadband services. Free-space links are affected by atmospheric turbulence which prompts fading and path loss resulting in reduction of coverage distances. While, optical fiber technologies also induce dispersion and non-linearity effects which require compensation technique.

The OFDM and DP-QPSK are seen multilevel modulation techniques for long and short distance transmission system in both direct and coherent detection, because DP QPSK provides very good noise immunity while OFDM is capable of many optical fiber limitations such as polarization mode dispersion (PMD) and chromatic dispersion (CD).

A hybrid optical fiber/FSO network system needs to minimize the separate fiber link and FSO link high data transmission systems which give complementary option one to another and mitigate the drawbacks. And also different advanced modulation techniques should be applied to reduce the transmission restrictions and transmit higher data rate signals at a time per single channel.

1.3 Objective of the Thesis

1.3.1 General objective

The main objective of this thesis is to design, simulate, and analyze the performance of a hybrid optical fiber/FSO communication system for high data rate transmission using coherent optical DP-QPSK and OFDM modulation techniques.

1.3.2 Specific objectives

The specific objectives of this paper are:

- ✓ To analyze the performance of CO-DP QPSK and CO-OFDM based hybrid optical fiber/ FSO systems with fiber nonlinearity effects.
- ✓ To analyze the performance of CO-DP QPSK and CO-OFDM based hybrid optical fiber/ FSO systems with fiber dispersion states.
- ✓ To investigate and simulate the CO-DP QPSK and CO-OFDM hybrid systems to carry 100Gbits/s with the OptiSystem simulation tool.
- ✓ Finally bit error rate and the Q-factor were verified to study the performance of the hybrid optical fiber/FSO system.

1.4 Literature Review

The use of optical bands can relieve the problems caused by spectrum shortage in radio frequency based wireless communication. Nowadays, researchers are trying to adapt many applications based on hybrid optical/wireless communications.

Advanced modulation formats play an important role in the design of high-speed short-range and optical access networks where high capacity, low cost, and minimum energy consumption are key for practical deployment.

In order to meet the objective, the reviews will be carried out in the following contexts:

- ➢ Hybrid optical fiber and free space wireless high speed data transmission
- ➢ Short range Multi-Mode Optical Fiber transmission
- ➢ Loss analysis for optical fiber transmission
- ➢ Performance of advanced modulation schemes.

In paper [1], the authors present a hybrid optical fiber/FSO Communication system for high-speed data transmission. Advanced DP-QPSK modulation format is applied to extend the transmission distances for both fiber and free-space communication. But it did not consider the implementation cost and energy consumption of the links. And also the coverage area can be increased further by applying multilevel advanced modulations like M-QAM, OFDM, and CAP, etc.

In paper [2], the authors present a high-capacity integrated optical-wireless communication system using advanced optical and wireless technologies. From the service aspect, gigabit mm-wave services provided by radio over fiber (RoF) systems have been demonstrated with the co-existence of legacy microwave services. A low-complexity UDWDM and QAM-OFDM modulation techniques are applied. Besides QAM and OFDM modulation formats, DP-QPSK and CAP modulations can be applied to the low complexity of the links.

It allows a relatively high data rate achieved by electrical and optical components of limited bandwidth and thus fits in the optical-wireless access network applications.

In paper [3], the author describes the design of underwater optical wireless communication (UOWC) transmitter optimized for modularity, cost, power consumption, and speed. The aim is to create and evaluate a system with a low enough cost and power consumption to allow for the inclusion of UOWC in projects of any size. The design should also be simple enough that the system is easy to expand or adapt to a specific project's needs.

The design uses light-emitting diodes (LEDs) as the optical generator to limit the power consumption. The system applies a Pulse Position Modulation (PPM) scheme that reduces the data throughput of the system.

Besides the PPM modulation scheme, other advanced modulation techniques can be applied to the low-complexity IM-DD links which allow relatively high data rate achieved by optoelectronics components of limited bandwidth, and thus fits in the optical-wireless access network applications.

In paper [5], the authors present a high-capacity optical network system for short distance communication. The paper focuses on fiber access network with the signal propagation distance of tens of kilometers and optical data center networks (ODCN) with distance of a few kilometers.

Furthermore, different advanced modulation formats has been also studied and transmission performance of both pulse amplitude modulation (PAM) and discrete multi-tone (DMT) signals in a short-reach optical link has been experimentally investigated. But to meet the low-cost requirements in short-haul communications and low power devices are preferred in both fiber access networks and data center networks (DCNs), other advanced modulation techniques, and optoelectronics components should be investigated.

1.5 Thesis Outline

This thesis will be divided into six chapters.

In the first chapter, the introduction and literature review of a high data rate hybrid optical fiber/FSO communication system will be described.

In chapter 2, advanced modulation techniques will be covered.

In chapter 3, optical communication system will be covered.

In chapter 4, the hybrid optical fiber-wireless communication system architectures are realized and illustrate the performance of the optical fiber/FSO hybrid system with OFDM and DP-QPSK modulation schemes. MATLAB software and OptiSystem simulation tool are used to design and simulate the system. In addition, this chapter discusses the simulation results and the analysis of the proposed systems.

In the last section, the work is concluded and future tasks will be discussed.

1.6 Scope of the Thesis

The scope of the thesis covers the design, simulation and performance analysis of a hybrid optical fiber/FSO communication system using coherent optical DP-QPSK and OFDM modulation techniques for 100Gbits/s data rate transmission.

CHAPTER TWO

Advanced Modulation Techniques

2.1 Introduction

Nowadays, the huge demand for broadband network services involves data communication systems to have an intensive capacity which subsequently improves the need for higher data rates. Increasing the number and employment of multiple optical components can improve the system carrying capacity, but for such desired systems the cost will increased as well. Therefore, another mechanism which is an advanced modulation format using a single wavelength channel has become a preference to improve spectral efficiency with similar optoelectronic components.

Multilevel modulation techniques such as multiple quadrature amplitude modulation (M-QAM), M-ary phase-shift keying (M-PSK), discrete multi-tone (DMT), and orthogonal frequency division multiplexing (OFDM) has been explored extensively [12, 13]. For the new generation optical communication systems, multilevel modulation formats have been stated to show many technical solutions. Therefore, an optical network system will be more realistic and effective if the employment of advanced modulation techniques can reduce the complexity of the system while simultaneously enhance spectral efficiency.

Among all other advanced modulation techniques, dual-polarization quadrature phase-shift keying (DP-QPSK) is one of the most important techniques for multi-Gbits/s or higher bit rate transmission. It consists of two orthogonal polarization states of the light signal with I/Q QPSK modulators and capable of encoding 4 bits/symbol rate at a time. The DP-QPSK represent light output in to symbols for minimizing the bandwidth of the transmission information and the symbols are encoded in both phase and polarization [13].

Orthogonal frequency division multiplexing (OFDM) is one of the well-known multiplexing techniques is the orthogonal frequency division multiplexing (OFDM) which encodes signals on multiple carrier frequencies. It has established into a popular scheme for broadband digital communication, applied in different streams like wireless networks, digital subscriber line (DSL) Internet access, power-line networks, and fourth generation (4G) mobile communication applications. The two fundamental advantages of OFDM are robustness against channel dispersion and its ease of phase and channel estimation in a time-varying environment. It has two

vital benefits which are robustness against channel dispersion and ease of phase and channel estimation in a time-fluctuating environment. In optical domain, OFDM has been widely studied to compensate for dispersion effects [21-23]. However, OFDM also has demerits such as sensitivity to frequency and phase noise signals, high peak to average power ratio (PAPR).

2.2 Dual Polarization-Quadrature Phase-Shift Keying Modulation

2.2.1 Principle of QPSK Modulation Format

In quadrature phase-shift keying (QPSK), commonly, a sinusoidal waveform is considered with phase variation while keeping the amplitude and frequency unchanged. Let the QPSK waveform can be expressed as shown in equation (2.1) [13, 14]:

$$S_{PSK}(t) = A\cos[\omega_c t + \theta_0 + \theta_i(t)] \quad (2.1)$$

Where S_{PSK} is the i^{th} phase PSK signal, A is the peak amplitude, ω_c is the carrier frequency ($\omega_c = 2\pi f_c$), θ_0 is the reference phase angle, θ_i represents the phase difference where i = 1, 2, 3, or 4. Two different BPSK systems (i.e $\cos \omega t$and $\sin \omega t$), one to the I-in phase and the other to the Q-quadrature, can generate QPSK signal which has the similar performance but the bandwidth of the system will be double.

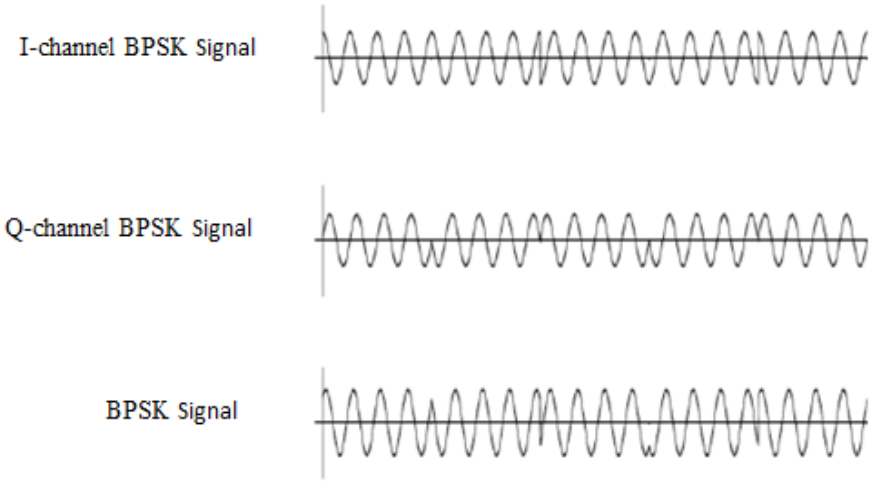

Figure 2 1: The generations of QPSK signal from two BPSK signals.

2.2.2 Optical DP-QPSK Modulation

As shown in figure 2.2, a DP-QPSK system is a combination of two QPSK systems in a polarized state. It uses two polarizations (i.e horizontal and vertical) with the identical QPSK constellation to assign the digital bits. The desired symbol rate can be decreased by four times which narrows the signal spectrum, reduces the speed required of an optical signal, and allows lower-cost applications. The dual polarization is performed at the optical carrier laser beam output with beam splitter. Thus, the DP-QPSK is a multilevel digital modulation format used in the optical communication systems with vertical and horizontal polarization the laser beams.

By default, the laser source is a continuous wave single polarization and let us considers it is horizontally polarized. To produce vertically polarized signals having equal power a beam splitting technique is required. The beam splitter gives two signal outputs one to the upper and the other is to the lower QPSK modulator with the same power. And then, either of the two parts is sent to polarization rotator, i.e in this case the upper part to make vertically polarized signal. Finally, the horizontally polarized signal is combined with the vertical polarized QPSK signal to get a DP-QPSK modulated output signal.

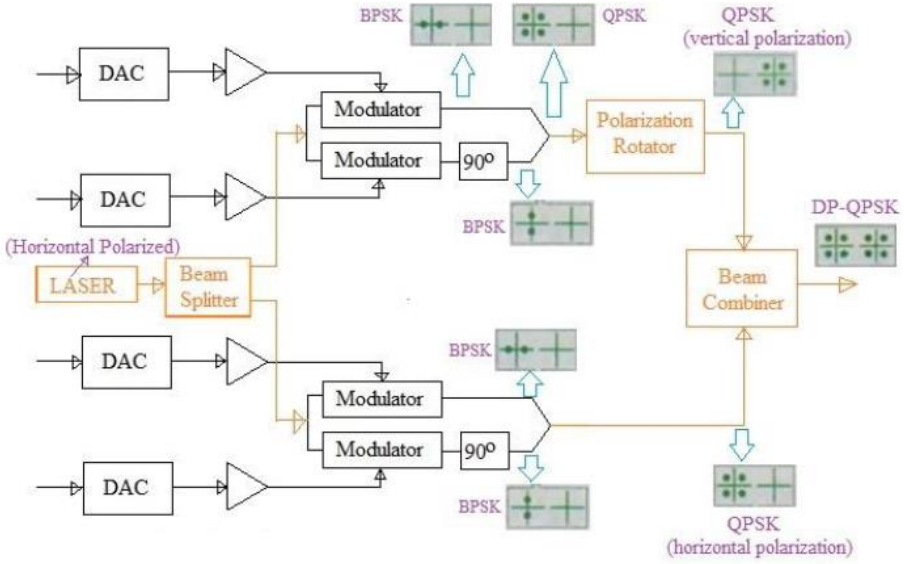

Figure 2 2: Block diagram of DP-QPSK modulator

A linearly polarized continuous light wave comes from a laser diode (LD) is an input into a DP-QPSK modulator [16]. Let the output of the LD can be expressed as:

$$E_{LD}(t) = \sqrt{P_{INo}}\exp[j(\omega_c t + \varphi)] \tag{2.2}$$

Where P_{INo} represent the average input optical power, ω_c is the carrier frequency, and φ represents the initial phase.

Most commonly, the modulation process of the DP-QPSK signal is done using an electro-optic mechanism with the Mach–Zehnder modulator working principles [15, 16]. Figure 2.2 shows the detailed structure and working principles of a DP-QPSK modulator. A single DP-QPSK modulator mainly consists of a polarization rotator and two DP-MZM modulators. A DP-MZM can be formed by connecting two MZMs in parallel or series. The electric field transfer function of an MZM biased is shown in equation 2.3 [15, 17]:

$$E_{MZo,PSK}(t) = jE_{LD}(t)\cos\left[\pi\frac{v_1(t) - v_2(t)}{2v_\pi}\right]\exp(j\beta l) \tag{2.3}$$

Where β represents the modulation constant of the MZM, v_π is the half-wave voltage of the MZM, $v_{1,2}(t)$ are the driving voltages of the modulator, and l represents the length of the each MZM electrode. In equation 2.3, $\varphi_{I,Q,PSK} = \pi\frac{v_1(t)-v_2(t)}{2v_\pi}$ is the baseband QPSK signal. Each DP-MZM is biased on one arm to give a 90^o phase shift. Thus, the DP-MZM output signal can be expressed as:

$$E_{MZo,PSK}(t) = jE_{LD}(t)\left[\cos(\varphi_{I,PSK}t) + \cos(\varphi_{Q,PSK}t)\exp(j\pi/2)\right]\exp(j\beta l) \tag{2.4}$$

Finally, the output of the optical modulator is transmitted through an optical fiber/FSO hybrid link and reaches at the receiver for further process. At the receiver, a DP-QPSK demodulator is mainly composed of four pairs of balanced photodiodes and two dual-polarization delay-line interferometers (DP-DLIs). Each dual-polarization delay-line interferometer consists of two Mach-Zehnder DLIs each has a phase shift on one arm and an exact one-symbol-period differential delay on the other [14, 18].

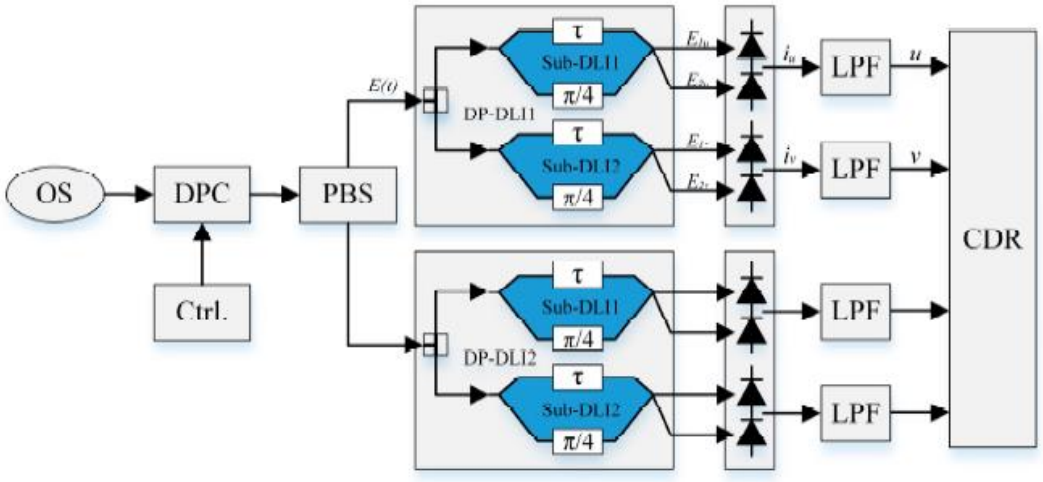

Figure 2 3: A schematic diagram of DP-QPSK receiver delay-line interferometer (DLI).

The output of the FSO link a polarization beam splitter (PBS) with laser beam source is applied to obtain two mutually orthogonally polarized signals.

At the receiver, the input to each DP-DLI is separated single-polarized signals, which transforms the phase-difference information into intensity information. After conversion, the intensity information is sent to balanced photodiodes and the noise is eliminated by applying filters. The original data is recovered using subsequent process. Assuming the responsivities (μ) of all photodiodes are the same, τ is the differential delay, and the signal at the input of DP-DLI is $E_{i,PD,PSK}(t) = Bexp[j((\omega_c t + \varphi) + \varphi_n)$, then the output of the DP-DLI can be derived as:

$$E_{1u,2u,1v,2v} = \frac{j}{2}[E_{i,PD,PSK}(t)e^{\pm j\pi/4} \pm E_{i,PD,PSK}(t-\tau)] \tag{2.5}$$

Based on the properties of the square-law of photodiodes, the converted photocurrent can be expressed as:

$$i_{PD,PSK}(t) = \frac{\sqrt{2}\mu B^2}{4}(\sqrt{2} + \cos\Delta\varphi_s - \sin\Delta\varphi_{LD2}) \tag{2.6}$$

After the process of balanced detection, the output electrical signals can be expressed as:

$$i_u(t) = \frac{\sqrt{2}\mu B^2}{2}(\cos(\Delta\varphi_S - \Delta\varphi_{LD2})) \tag{2.7}$$

$$i_v(t) = \frac{\sqrt{2}\mu B^2}{2}(\sin(\Delta\varphi_S - \Delta\varphi_{LD2})) \tag{2.8}$$

$$I_I(t) = R\left\{\sqrt{P_S P_{LO}}(\cos(\Delta\varphi_S - \Delta\varphi_{LD2})\right) and\ I_Q(t) = R\{\sqrt{P_S P_{LO}}(\sin(\Delta\varphi_S - \Delta\varphi_{LD2})) \tag{2.9}$$

Where $\Delta\varphi_{S,LD2}$ is the phase difference between adjacent symbols, P_S is the power of the transmitted signal and P_{LO} is the power of the coherent detection local oscillator.

Finally, the amplified signal is passed to a digital signal processor (DSP) to equalize the transmission impairments such as group velocity dispersion and phase mode dispersion of optical fiber.

2.3 Orthogonal Frequency Division Multiplexing Technique

2.3.1 Working principles of OFDM

As shown in figure 2.4 below, the OFDM technique consists of a transmitter that split into multiple parallel streams. Each carrier signal is mapped using QAM or PSK modulation scheme symbol stream.

After mapping, the symbol streams are modulated onto the multiple carriers using IFFT to transform the signal from the frequency to time domain. A guard interval or cyclic prefix is added to avoid the overlapping between multiple carriers after IFFT operation, and then the signal is fed to a digital to analog converter (DAC). At the receiver, the cyclic prefix or guard interval is removed to recover the original signal. Then the signal is demodulated by using the FFT algorithm and QAM or PSK demodulator. Finally, the data is converted from parallel to serial to get the original data stream [21, 24].

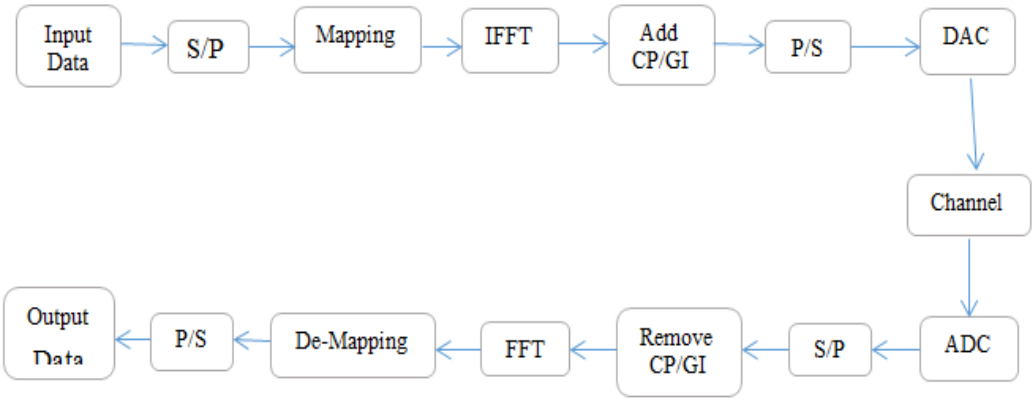

Figure 2 4: Block Diagram of OFDM system

2.3.2 Optical OFDM modulation

In optical fiber communication systems, OFDM emanates into two senses, namely coherent detection optical OFDM (CO-OFDM) and direct-detection optical OFDM (DDO-OFDM) [25, 27]. Direct detection OFDM is recognized by sending the optical carrier signal along with the OFDM band and a single photodiode can be made at the receiver side to convert the optical field back into the electrical domain whereas, in coherent detection, the optical carrier signal is suppressed and the receiver is realized by coherent detection with a local oscillator or laser diode (LD).

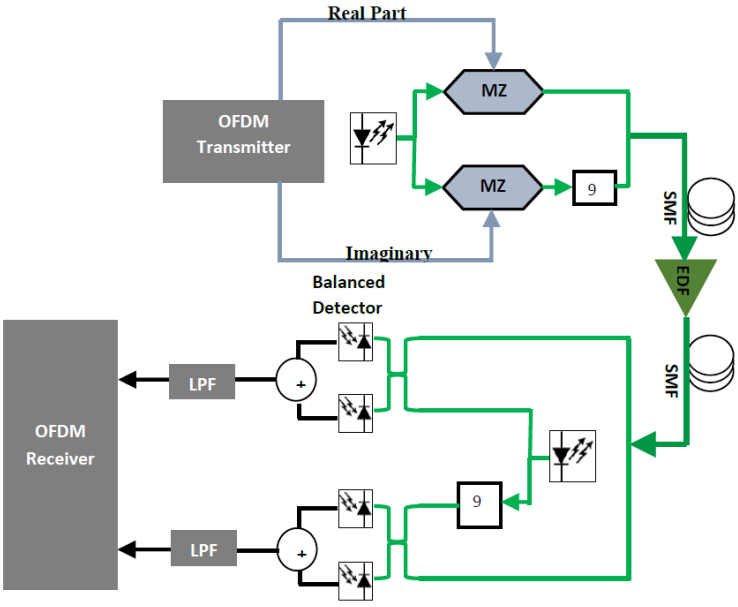

Figure 2 5: Block diagram of a general CO-OFDM systems

The CO-OFDM has greater performance with optical signal-to-noise ratio (OSNR) requirements, PMD tolerance, and spectral efficiency for long-haul communication systems, whereas direct detection is more appropriate for cost-effective short-distance broadband services.

The main demerits of coherent detection are polarization dependent and very sensitive to phase noise of the laser diode. Since it incorporates the advantages of both coherent detection and OFDM techniques, CO-OFDM are the new-generation technology for optical communications. [30]. In CO-OFDM the optical carrier is generated from a local oscillator at specific wavelengths. Depending on the frequency of the laser diode, the coherent optical detection can be categorized as heterodyne or homodyne detection.

When the frequency of the output of the local oscillator (LO) does not match the incoming optical signal frequency it is called heterodyne detection. At the receiver end, the second laser output and the incoming signals are mixed to generate a new signal with intermediate frequency (IF). Heterodyne technique will decrease the shot and thermal noise which improves SNR performance of the system. However, the received optical source frequency will disposed to drift over time and the IF has to be regularly checked, and the local oscillator frequency must be improved to keep the IF constant.

For the analysis of the coherent optical OFDM system we consider two tone models. The two complex subcarrier tones can be expressed in equation 2.10 and 2.11 [31, 32]:

$$S_1(t) = Ae^{j2\pi f_1 t} \tag{2.10}$$

$$S_2(t) = Ae^{j2\pi f_2 t} \tag{2.11}$$

Where A represents the rms value, $f_{1,2}$ represent the frequencies of the two tones.

And also the optical carrier signal generated from the LO at the input of the modulator can be expressed as:

$$E_{LD}(t) = \sqrt{P_{INo}}\exp[j(\omega_c t + \varphi)] \tag{2.12}$$

And let $s_{12}(t)$ is the complex electrical signal produced by mixing the two tones:

$$S_{12}(t) = V_{I,12} + V_{Q,12} = A(\cos 2\pi f_1 t + \cos 2\pi f_2 t + j(\sin 2\pi f_1 t + \sin 2\pi f_2 t)) \tag{2.13}$$

Assuming that, the MZM is in unbiased condition which is optimal, the initially $\varphi = 0$, and the nonlinearities are insignificant; the optical modulator output can be expressed:

$$E_{MZo,OFDM}(t) = E_{LD} M S_{12}(t) e^{j\omega_c t} \tag{2.14}$$

Where E_{LD} represents the rms value of the laser output with frequency f_c, the factor $M = A \times \frac{\pi}{2V_\pi}$, V_π represents the half-wave switching voltage of each MZM.

Practically, the complex input signal and all the input voltages of the LiNb-MZM contribute for the variations of both amplitude and phase of the modulator output [33]. The LiNb-MZM output optical field can be expressed by equation 2.15 [34]:

$$E_{MZo,OFDM} = \frac{E_{LD}}{10^{(\frac{L_{ins}}{20})}}[\gamma e^{(j\frac{\pi A_2}{V_{\pi RF}} + j\frac{\pi A_{b2}}{V_{\pi DC}}} + (1-\gamma)e^{(j\frac{\pi A_1}{V_{\pi RF}} + j\frac{\pi A_{b1}}{V_{\pi DC}}}] \tag{2.15}$$

where L_{ins} represents the parameter insertion loss, A_1 and A_2 are rms input electrical voltage for the lower and upper modulator arms, A_{b1} and A_{b2} are bias voltage 1 and voltage 2, $v_{\pi RF}$ and $v_{\pi DC}$ are the bias and switching modulation voltages, and γ denoted the power splitting ratio of

both Y-branch waveguide (assumed to be symmetrical), and $\gamma = \frac{1-\frac{1}{\sqrt{\varepsilon_r}}}{2}$ Where $\varepsilon_{r=10^{exr/10}}$ and exr is the extinction ratio equal to the P_1/P_2, where $P_{1,2}$ is average power outputs.

The transmitted light intensity is detected at the end of the transmitting link and the original data is recovered through the down conversion procedures. Assuming linearity in every signal processing stages and negligible optical hybrid loss, the transmitted signal and the second LO optical signal are mixed together to form a coherent detection. Each optical detector has two couplers and two PIN photo diodes.

The output electrical field of the four 90^o optical hybrid ports can be expressed by equation 2.16 and 2.17 [38]:

$$E_{1,2,} = \frac{1}{\sqrt{2}}[E_s \pm E_{LD2}] \tag{2.16}$$

$$E_{3,4} = \frac{1}{\sqrt{2}}[E_s \pm jE_{LD2}] \tag{2.17}$$

Where E_s, E_{LD2} are the received signal at the end of the link and local oscillator signal (LO) at the receiver side respectively.

The real value of the output photo-current can be recovered by using the two photo-detectors (PD1, PD2):

$$I_{1,OFDM} = |E_1|^2 = \frac{1}{2}\{|E_s|^2 + |E_{LD2}|^2 + 2Re\{E_s {E_{LD2}}^*\}\} \tag{2.18}$$

$$I_{2,OFDM} = |E_2|^2 = \frac{1}{2}\{|E_s|^2 + |E_{LD2}|^2 - 2Re\{E_s {E_{LD2}}^*\}\} \tag{2.19}$$

$$|E_s|^2 = |E_r|^2 + |n_o|^2 - 2Re\{E_s {n_o}^*\}\} \tag{2.20}$$

$$|E_{LD2}|^2 = I_{LD2}(1 + I_{rin}(t)) \tag{2.21}$$

Where $I_{LD2}, I_{rin}(t)$ represent the rms power and relative intensity noise of the LD. Due to the balanced photo-detection, the real component of the photo-current becomes [39]:

$$I_I = 2Re\{E_s {E_{LD2}}^*\} \tag{2.22}$$

$$I_Q = 2Re\{E_s {E_{LD2}}^*\} \tag{2.23}$$

Based on equations (2.18) and (2.19) the complex photo-current can be expressed by:

$$I_{OFDM}(t) = I_I(t) + jI_Q(t) = 2E_s E_{LD2} \tag{2.24}$$

After the optical detection process, the received signal is transmitted to the OFDM receiver to recover the original signal.

CHAPTER THREE

Optical Communication Systems

3.1 Introduction

Multi-gigabits/s and beyond data rate broadband services are evolving continuously to meet the demand for wireless capacity of the new generations. The current RF spectrum is facing a challenge to meet the demand of future high data rate networks. Due to its ultra-wide range of unregulated spectrum, optical wireless communication (OWC) has emerged as capable to overwhelm the RF spectrum shortages.

Optical fiber communication has been the leading technology for the past decade for higher data communications over long-haul and medium distances. However, for short distances, transmitting data over optical fibers have some technological demerits. As a result, optical fiber communications have not been able to provide network services such as chip-to-chip and board-to-board communication. Nowadays, many researchers have been working on free-space optical (FSO) communication to mitigate the fiber optic drawbacks. The working principle of FSO is essentially the same as that of fiber optic transmission. But, FSO uses air as a transmission medium and light travels through air faster than it does through glass for less distance. Even though optical fiber is the most reliable way to provide high data rate optical communications; the digging, delays, and related costs to lay fiber make it very expensive. Moreover, once the fiber is deployed, it cannot be re-deployed if a customer needs to relocate or shift to another service provider, making it extremely difficult to recover the asset in a reasonable timeframe. Furthermore, most of the recent networks to deploy fiber have been to improve the metro core (backbone), while the access and end-user have completely been ignored. FSO technologies can offer effective and cost-wise last and first mile services by connecting to fiber backbone infrastructure directly to end customers. FSO network is designed with short optical links (typically range from 200 to 2000 m), whereas fiber optic cable can be used for the long-haul (up to 200 km without repeaters or regenerators). It can also promise high connectivity and overcome optical fiber restrictions such as dispersion and PMD [41, 42].

3.2 Optical Fiber Links

3.2.1 Optical fiber

Fiber optic is a field of applied science and engineering that deals with the design and application of optical fibers. An optical fiber is a flexible, transparent wire made of extruded glass (silica) or plastic, which can role as a waveguide to transmit light between the two ends of a fiber cable.

Optical fiber typically contains a transparent core bounded by a lower refractive index cladding material. When a ray of light strikes a medium boundary at an angle greater than a particular critical angle with respect to the normal surface, the transmitted light is kept in the core by total internal reflection. If the refractive index of the cladding material is lower than the core and the incident angle is greater than the critical angle, all of the light is reflected and the fiber acts as a waveguide [43].

Practically, if optical communication applies fiber medium, every phone, smart sensor, and the mobile device could be directly connected to the fiber backbone but that would limit the mobility of the devices. Fibers are used instead of copper wires because signals travel along with them with less attenuation and are also immune to electromagnetic interference. Fibers are also used for illumination and are wrapped in bundles so that they may be used to carry images, thus allowing viewing in confined spaces. Specially designed fibers are used for a variety of other applications, including sensors and fiber lasers.

According to the number of propagating light signals, fibers can be categorized into two. The first one is the single-mode fiber which supports one light signal at a time. The second type supports many propagation paths or transverse modes known as multi-mode fibers (MMF). Generally, MMF has a wider core diameter and can transmit high power signals for short-distance communication links, whereas single-mode fibers are mostly used for long-distance communication links.

In transmitting the optical signal over a fiber cable, the main concerns are transmitting the signal without distortion and with small attenuation. Silicon-based optical fiber can transmit the light wave with loss (attenuation) equal to 0.2dB/km. However, for long-haul transmission, the fiber loss increases every 100km by 1%. Hence, in designing an optical fiber, the fiber loss must be considered to determine the space between amplifiers for the system.

Another optical fiber drawback that must be considered in designing of a fiber system is the dispersion effect that leads to the light pulse broadening and makes it hard to recover the original signal accurately.

The fiber dispersion can occur severely in the MMF but less in the case of SMF, which makes the single-mode fiber more suitable for the communication systems design, especially for long-haul applications.

3.2.2 Fiber attenuation

The primary function of a fiber link for a range of applications is efficient transmission of light at operational wavelengths. As light propagates through a fiber, the intensity will reduce after a certain fiber length known as attenuation. In fiber system design, the signal intensity degradation can be strengthening through amplification, interconnect optimization, fiber geometry design, and environmental isolation. An understanding of attenuation mechanisms and the potential for their minimization is, thus, of great importance in the efficient and economic use of fiber optics.

Attenuation, also known as fiber loss, transmission loss, and power loss, and can determines the maximum repeater less separation between a transmitter and receiver. An attenuation unit is dB/km and, in an optical fiber, the main cause of attenuation is absorption, scattering, bending, and Core-Cladding.

Figure 3 1: The effect of attenuation

The total optical throughput of an optical fiber with external MZM can be quantified in terms of the input optical power($P_{out,MZM}$) which equal to the MZM output power and the output power ($P_{out,fiber}$) received after light propagates a fiber length (L) and expressed in equation 3.1 [44]:

$$P_{out,fiber} = P_{out,MZM} e^{-\alpha_{tot} L} \tag{3.1}$$

$$\alpha_{tot} = \frac{10}{L} \log \frac{P_{out,fiber}}{P_{out,MZM}} \tag{3.2}$$

Equation 3.1 is referred to as Beer's Law and shows that transmitted power decreases exponentially with propagation distance through the fiber, and α_{tot} is the total attenuation coefficient (i.e. involving all contributions to attenuation).

Attenuation depends on the wavelength of light. Silica fiber exhibits a minimum loss of about 0.2dB/km near 1.55nm wavelength, and it is higher at shorter wavelengths, reaching a level of a few dB/km in the visible region [49].

a. Optical absorption

Optical absorption is a process in which the light energy is directly transferred from the propagating light beam to the material structure, resulting in the excitation of the material's energy state. The energy absorption promotes the oscillator to a higher energy level which, in turn, gives rise to the complex refractive index of the material at optical frequencies. OH ions (water) are the main absorption factors in the presence of fiber material impurities. The low absorption regions are between these wavelengths. For standard single-mode fiber, at 1310 nm, the attenuation is 0.4dB/km and, at 1550nm, the attenuation is 0.25dB/km. Both frequencies lie at the low water peak regions. However, for standard single-mode fiber at around 1440nm, the E-band water molecules cause high attenuation (high water peak) [49, 50].

In the last few years, manufacturers of fiber are working to produce a low-water-peak fiber to minimize the water peak area especially at the E-band (1360-1460nm).

b. Optical scattering

Optical scattering is a state of changing the propagation direction, phase, and polarization of photons due to the dielectric medium. If the light propagates without energy loss and the photon frequency after scattering remains the same, the process is called an elastic scattering process. These spatial variations in the dielectric constant are usually localized and are called scattering centers. Scattering centers are associated with extrinsic, second-phase impurities or intrinsic fluctuations in material composition. Currently, silica glass fiber production largely excludes the formation of extrinsic sources of scattering. Intrinsic scattering attenuation effects play the dominant role in telecommunications grade fiber systems. Primary sources of elastic scattering arise from Rayleigh and Mie scattering in the fiber materials. Scattering losses occur when

material density microscopically variations, compositional fluctuations, and defects during the fiber production process.

c. Bending losses

In addition to absorption and scattering losses within the glass components of the fiber, the fundamental characteristics of light propagation within the fiber design coupled with the uniformity and control of fiber parameters also present factors contributing to the optical loss.

Propagating modes within an optical fiber can be characterized by an electric field distribution with maxima inside the fiber core and evanescent fields that extend outside the fiber core into the cladding. Thus, some of the optical energy in the mode is propagating in the cladding.

d. Core and cladding loss

When the fiber components i.e the core and the clad have no homogenous medium, different intensity levels at a given fiber distance will be observed. For a step-index fiber, the effective attenuation will be weighted according to the fraction of the optical power transmitted in each material (i.e. core vs. clad). The loss associated with a mode indices ν, m of a step-index fiber:

$$\alpha_{vm} = \alpha_1 \frac{P_{core}}{P} + \alpha_2 \frac{P_{clad}}{P} \tag{3.3}$$

Where $P_{core,clad}/P$ represents the fractional power carried in the core and cladding regions; P is the total power transmitted; $\alpha_{1,2}$ represents attenuation coefficients for the core and cladding, respectively.

The average power will be the sum of the fractional powers for each propagating mode. A more complicated mathematical analysis involving the radial behavior of the refractive index is used for graded-index fibers.

3.2.3 Fiber dispersion

When light travels along a fiber cable, the signal shape will broaden which is called fiber dispersion. It leads the pulse to overlap with the closer pulses or eventually make it hard to recover the original signal accurately and reduces the capacity of a fiber link Bandwidth.

Chromatic dispersion and polarization mode dispersion are some of the different types of signal dispersion that can occur during the transmission of a signal.

Figure 3 2: Effect of dispersion

a. Chromatic Dispersion

Chromatic dispersion has occurred when the pulse broadening happens in a single-mode fiber. The main cause of chromatic dispersion is the finite spectral width of the optical source. It depends on the wavelength of the light signal and can be defined as:

$$D = \frac{1}{L}\frac{\partial \tau_g}{\partial \lambda} = \frac{\partial(1/v_g)}{\partial \lambda} = \frac{-2\pi c}{\lambda^2}\beta_2 \tag{3.4}$$

Where D represents the dispersion, L represents the pulse traveling fiber distance, $\frac{\partial \tau_g}{\partial \lambda}$ represents the delay difference per wavelength to propagate the fiber distance L, v_g represents the group velocity, c is the speed of light, β_2 is the GVD (Group Velocity Dispersion) parameter. $\beta_2 = \frac{\partial^2 א}{\partial \omega^2}$, where א is the wave propagation constant/coefficient and ω is the angular frequency [50]. Chromatic dispersion is caused by material dispersion and waveguide dispersion.

1. Material dispersion

Material dispersion is happed when the refractive index of the core material of the fiber varies with the change of the light wavelength. Material dispersion can be defined as [50-52].

$$|D_{mat}| = \frac{\lambda}{c}\left|\frac{\partial^2 n}{\partial \lambda^2}\right| \tag{3.5}$$

Where D_{mat} represents the material dispersion, and n represents the refractive index of the core.

2. Waveguide dispersion

Waveguide dispersion is another type of chromatic dispersion. Waveguide dispersion depends on the optical fiber core diameter and it causes signals of different wavelengths to travel at different velocities. As a result, the pulse will spread and make it overlap with neighboring pulses.
Mathematically, waveguide dispersion can be defined as:

$$D_{wg} = -\frac{n_1 \lambda \Delta}{c} \frac{\partial^2 d}{\partial \lambda^2} \tag{3.6}$$

Where d is the diameter of the fiber core.

b. Polarization mode dispersion

When the polarization state of an optical signal is changed due to the fiber birefringence, then pulse broadening will occur. Imperfections from the manufacturing process, the bending or twisting of the fiber, or weather conditions are some of the factors that can cause fiber birefringence. Because of birefringence, at specific wavelengths, signal energy takes two polarization modes with different velocities. The difference between the two polarization modes will produce pulse spreading.

$$\Delta\tau_{PMD} = \left| \frac{L}{v_{gx}} - \frac{L}{v_{gy}} \right| \tag{3.7}$$

Where L represents the distance that the pulse travels and v_{gx}, v_{gy} are the group velocities of the two polarization mode. The polarization-mode dispersion (PMD) can be calculated by:

$$D_{PMD} \approx \frac{\Delta\tau_{PMD}}{\sqrt{L}} \tag{3.8}$$

3.2.4 Fiber nonlinear impairments

The fiber dispersion is not the only factor to degrade the optical signal strength and affect the transmission process. The optical signal can be subjected to fiber nonlinearity effects though out the transmission links. The Kerr nonlinearity and the stimulated elastic scattering process are the two fiber nonlinear impairments types.
The Kerr nonlinearity is occurred from the fiber refractive index which is dependent on the intensity of the propagated signal. This can be expressed as [53]:

$$\emptyset(\omega, |E|^2) = n(\omega) + n_2 |E|^2 \tag{3.9}$$

Where n_2 represents the nonlinear index coefficient, ω is the angular frequency.

The three important Kerr nonlinearity effects are self-phase modulation (SPM), cross-phase modulation (XPM), and four-wave mixing (FWM).

The stimulated elastic scattering is happened when the energy transfer from the optical field to the medium. It includes two types: Stimulated Raman Scattering (SRS), and Stimulated Brillouin Scattering (SBS).

a. Self-phase modulation (SPM)

In SMF, when an ultra-short light pulse propagates a varying medium refractive index will produced. Due to this variation, a phase shift on the light pulse will occur and lead to a change in the pulse's frequency. The nonlinear phase shift is proportional to the light intensity and can be expressed by equation 3.10 [54].

$$\emptyset_{NL}(L,T) = n_2 k_0 L|E(L,T)|^2 \tag{3.10}$$

$$\omega(t) = \omega_0 + \left(\frac{4\pi n_2}{\lambda_0 \tau^2} L \frac{P_{out,fiber}}{A_{eff}}\right) * t$$

Where $\emptyset_{NL}$ represents the nonlinear phase shift, n_2 is the nonlinear refractive index, L is the length of the fiber, $E(L,T)$ represents the electrical field at L distance, ω_0 is linear angular frequency, λ_0 linear wave length, τ is the time delay and $k_0 = \frac{2\pi}{\lambda_0}$ where k_0 is the wavelength of the signal, and A_{eff} is the area of the cross section of the beam into the fiber.

Generally, the SPM does not change the shape of the light pulses but broadens the spectrum of the optical pulse which will generate a frequency chirp to add a new frequency to the pulse.

When taking polarization into consideration, an array of new nonlinear effects can be predicted and nonlinear contributions to birefringence are given by [55]:

$$\Delta n_x = n_2\left(|E_x(L,T)|^2 + \frac{2}{3}\left|E_y(L,T)\right|^2\right) \tag{3.11}$$

$$\Delta n_y = n_2\left(\left|E_y(L,T)\right|^2 + \frac{2}{3}|E_x(L,T)|^2\right) \tag{3.12}$$

It is easy to see that the relative optical intensities in the x and y direction can affect the nonlinear birefringence. These two components interact nonlinearly in a way that is analogous to Cross-Phase Modulation (XPM), resulting in a relative nonlinear phase shift between the two components:

$$\Delta\emptyset_{NL} = \gamma L_{eff}(1 - B)(P_x - P_y) \tag{3.13}$$

Where $P_{x,y}$ represent the powers in the x and y components, respectively, and B is the ellipticity of the fiber (B = 2/3 for a linearly birefringence fiber). Such a relative nonlinear phase shift can be introduced by co-propagating a strong pump, polarized along the x-axis of the fiber, with a weak arbitrarily polarized signal. $\Delta\emptyset_{NL}$ determines the particular evolution of the polarization as the beam propagates and can, for instance, lead to a rotation of the polarization (optical Kerr effect) [55]. When taking the respective polarization of the two beams into account, XPM can also give rise to interesting temporal and spectral polarization effects. In a pump-probe situation, the probe polarization can be shown to rotate, with different parts of the pulse developed [56].

b. Cross-phase modulation (XPM)

XPM occurs when two or more optical pulses affect the phase and intensity of each other while broadening.

When two optical fields, E1 at frequency w1 and E2 at frequency w2, propagate through the fiber at the same time, the nonlinear phase shift is given by [56]:

$$\emptyset_{NL}(L,T) = n_2 k_0 L(|E_1|^2 + |E_2|^2) \tag{3.14}$$

Losses in fiber or signal attenuation will reduce peak power during transmission of optical signals inside the fiber as given in the formula below:

$$P_{out,fiber} = P_{out,MZM} e^{-\alpha L} \tag{3.15}$$

Where α is the attenuation constant and can be expressed as the unit of dB/km using the formula below:

$$\alpha = \frac{-10}{L} \log\left(\frac{P_{out,fiber}}{P_{out,MZM}}\right) \tag{3.16}$$

The effective link length, the length of EDFA, is obtained as:

$$L_{eff} = \frac{(1 - \exp(-\alpha L))}{\alpha} \tag{3.17}$$

The effective length after installing optical amplifiers with G and amplifier spaced distance z [i], is defined as: $L_{eff} = \frac{(1-\exp(-\alpha L^2))}{\alpha} \frac{L}{z}$

Nowadays, most of the works on linear and nonlinear impairments are based on a pump-probe analysis and linearization of the distortion around the signal.

For mathematical analysis, the starting point is the equation of transmission of light through optical fiber can be defined by the nonlinear Schrödinger (NLS) equation (eq.) which includes both nonlinear and dispersion effects [57, 58].

$$\frac{\partial B_j}{\partial z} + \frac{\alpha}{2} B_j + \frac{1}{v_{g-j}} \frac{\partial B_j}{\partial t} + i \frac{iD}{2} \frac{\partial^2 B_j}{\partial t^2} = i\vartheta(|B_j|^2) B_j \tag{3.18}$$

Where D is the linear dispersion, α is the attenuation coefficient, v_{g-j} represents the group velocity of the j^{th} wave, ϑ is the nonlinear coefficient, B_j is the electric field envelope of the transmitted wave. Assuming a continuous wave (CW) transmitted signal with the effect of fiber dispersion on the waveform is taken into account [59].

$$P_{j,out,fiber}(z, \omega) = |B_j(z, \omega)|^2 = P_{j,out,fiber}(0, \omega) \cos(qz) \exp(-\alpha z + i\, \omega z / v_{g-j}) \tag{3.19}$$

Where $q = \omega^2 D_j \lambda_j^2 / (4\pi c)$ with D_j and λ_j being dispersion coefficient and wavelength of the transmitter channel.

3.3 Free Space Optical Communication

The optical bands such as IR, UV, and VL are used for propagation in optical wireless communications (OWCs) systems. They have exceptional benefits, and numerous wireless technologies are based on them [60]. IR is invisible to people and applicable when lighting is not necessary. The optical wireless (OW) spectral regions have 750nm to 1 mm for IR, 380nm–750nm for VL, and 10nm–400nm for UV [61].

As a derivative of OWC, VLC is a type of wireless communication that uses unguided and unrestricted light to convey a signal.

The light signal is encoded and modulated with the modulated signal used to regulate the LED or LD transmitter, which can be pulsed at unnoticeable high speeds for the human eye. The signal transmitted by LED is detected by a photo-detector, usually a photodiode. The prospects of VLC are very wide-range from outdoor use such as vehicular networks to indoor personal area networks (PANs) [62, 63]. LEDs are broadly used for advertising displays, lamps, car lights, and home appliances, making use of VLC for short and medium-distance communications promising.

In free-space optics (FSO), the light pulse propagates in an open space. FSO can operate in VL, IR, and UV spectra and uses a very large frequency range when compared with the RF spectrum; therefore very high data rates can be achieved [64, 65].

But, FSO links are not reliable for long-range due to weather situations and physical obstructions like trees and buildings when they are in the line of sight of transmission. Optical camera communications (OCCs) are the OWC based technology used mainly in flashlights and cameras of smartphones. OCC uses either the IR or VL spectrum. Mostly, LEDs are used as transmitters and cameras as the receivers; as a result of the poor frame rates of cameras, this communications technique suffers from the low data rate.

Commonly, FSO link setup is used for multicasting purposes and can provide virtually unlimited bandwidth at relatively high performance and low-cost communication over short distances up to a few hundred meters. In addition, FSO links do not require any spectrum allocation by the Federal Communications Commission (FCC). These links are also easily deployable, scalable, and flexible.

The transmitted FSO signal is suffered from atmospheric and scintillation fading due to weather conditions and atmospheric turbulence. According to the FSO transmission formula the optical power of the signal is given by:

$$P_{r,FSO}(t) = C|E_r(t)|^2 = G_{total} L_{FSO} ב^X P_{out,fiber}(t) + P_{ASE} \quad (3.20)$$

Where $C = c\varepsilon_0/2F$: c represents the speed of light in air, ε_0 is the dielectric constant of the air medium and F represents the variable cross section of the Gaussian profile laser beam through the path of the mobile FSO link.

Where G_{total} represents the total optical gain due to the amplifiers in each transceiver of the link terminals $L_{FSO}$is the FSO link calculation which combines attenuation and geometrical aspects based on the equation below [66]:

$$L_{FSO} = \frac{{D_R}^2}{(D_T + \Delta\theta . L)^2} 10^{-0.1\alpha_{atm} L} \quad (3.21)$$

Where D_R represents the receive aperture diameter in m, D_T represents the transmit aperture diameter in m, $\Delta\theta$ is the beam divergence in mrad, L represents the link range in km and α_{atm} is the atmospheric attenuation factor in dB/km calculated via the formula below:

$$\alpha_{atm} = \frac{3.91}{V} (\lambda/550)^{-q} \quad (3.22)$$

Where V represents the visibility in km, λ is the wavelength of carrier in nm and q represents a parameter evaluated between 0-1.6, according to weather conditions. The ב factor tells the variation of the signal fading due to atmospheric turbulence and X has the value 1 or 0, in case of turbulence existence or not, respectively. Finally, P_{ASE}, is the overall power from Amplified Spontaneous Emission (ASE) of the amplifier stages.

For intensity scintillation, a Gamma-Gamma distribution [67, 68] is used to model atmospheric fading and the probability of a given intensity is:

$$P(I) = {2(ab)^{(a+b)/2}}\Big/{\Gamma(\alpha)\Gamma(\beta)} * I^{\left(\frac{a+b}{2}-1\right)} * K_{a-b}(2\sqrt{(abI)}) \tag{3.23}$$

Where 1/a and 1/b are the variances of the small and large scale eddies, respectively [a], Γ (.) is the Gamma function and K_{a-b} (.) is the modified Bessel function of the second kind.

$$a = \exp\left[\frac{0.49\sigma R^2}{(1+1.11\sigma R^{12/5})^{5/6}}\right] - 1 \tag{3.24}$$

$$b = \exp\left[\frac{0.51\sigma R^2}{(1+0.69\sigma R^{12/5})^{5/6}}\right] - 1 \tag{3.25}$$

The Rytov variance is: $\sigma R^2 = 1.23 {C_n}^2 K^7 Z^{11/6}$

Where ${C_n}^2$represents the parameter index refraction structure, K is the optical wave number and Z is the parameter Range. Channel time variations are considered according to the theoretical quasi-static model, also called the frozen channel model. By this model, channel fading is considered to be constant over the duration of a frame of symbols (Coherence time), changing to a new independent value from one frame to next. The coverage radial distance of a typical FSO system can be determined using equation 3.27 [43]. By considering the distance h and the beam divergence angle θ the incident light radius r can be expressed as:

$$r = h * \tan(\frac{\theta}{2}) \tag{3.27}$$

3.4 Hybrid Optical Fiber/FSO Links

Free space optics (FSO) is a line of sight optical communication for short-distance data transmission in both indoor and outdoor wide range of applications. It allows high bandwidth, unregulated spectrum, low infrastructure cost, and better security.

However, FSO links are sensitive to atmospheric turbulence which prompts fading and path loss resulting in limitations of coverage distances.

Optical fiber communication has been the leading technology for the past decade for higher data communications over long-haul distances with less attenuation and less electromagnetic interference (EMI).

However, for short distances, transmitting data over optical fibers have some technological demerits. As a result, optical fiber communications have not been able to provide network services such as chip-to-chip and board-to-board communication. It also induces dispersion and non-linearity effects which require compensation techniques.

In this paper, a hybrid optical fiber/FSO communication system is considered, designed, and simulated to compensate for the limitations of both fiber and free-space links. It can handle high-speed operations, multiple channels, long and distance data transmissions.

Along with the hybrid system, advanced modulation techniques (i.e BPSK, DPSK, QPSK, QAM, CAP, OFDM, etc.) are implemented at the transmitter and receiver section to enhance spectral efficiency for a good system performance. These modulations allow the transmission system to carry multi-Gbps or Tbps data rates per channel.

Figure 4.9 shows the block diagram of the proposed hybrid optical communication system. The hybrid optical fiber/FSO communication system consists of a transmitter, fiber/FSO links, and the receiver end. The transmitter consists of a binary signal generator, DP-QPSK/OFDM modulators, and RF to optical up-converter (RTO). The RTO is used to modulate the RF signal with a continuous wave laser optical carrier signal. The modulated optical signal is transmitted through the hybrid fiber/FSO channel to be coherently detected at the receiver. After each fiber span, an erbium-doped fiber amplifier (EDFA) is inserted to amplify the optical weak signal. At the receiver, the optical signal is received with an FSO receiver telescope, and then optical to RF (OTR) down-conversion is done using a photodiode.

Then, the signal is passed through a low pass cosine roll-off filter to eliminate the noise and to the QPSK/OFDM demodulator to recover the original signal.

And also the hybrid setup uses various visualizers such as an optical spectrum analyzer (OSA), for observing the optical signal spectrum, bit error rate (BER) analyzer for observing the eye diagram, Q-value, and BER of the system. The BER value acceptable is for an optical communication link. For error-free communications, the forward error correction (FEC) threshold that is the BER should be less than or equal to, which corresponds to a Q-factor of greater than or equal to 6.8. Thus all optical links with Q-factor greater than or equal to 6.8 are suitable for data communication [2, 6, and 21].

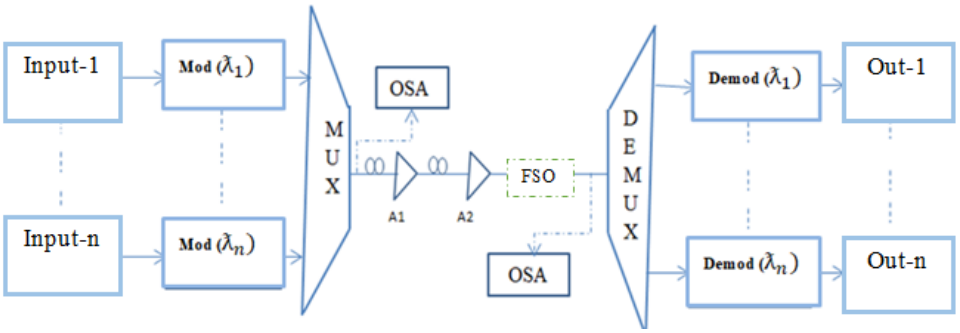

Figure 3 3: Block diagram of the hybrid optical multi-channel communication system model

3.4.1 BER analysis for CO-OFDM

To evaluate the bite error rate (BER) of an OFDM system it is important to consider the prefixes that are included in the OFDM modulator and the time window (or sequence length) of the simulation is temporarily extended beyond that defined by the global parameter settings. At the demodulator, the same prefixes are removed, the original sequence length is re-established; however, a portion of the information from the original data stream is lost. To avoid including this part of the bit stream within the BER calculation it is required to ignore a certain portion of the trailing bits from the original bit sequence.

Within the BER Analyzer this can be set within the parameter Ignore end Bits using the following formula:

$$\mathrm{Bits_{Ignore}} = \mathrm{S} - \mathrm{int}\left(\frac{\mathrm{n_{FFT}} * \mathrm{S}}{\mathrm{n_{Sub}} * \mathrm{Bits_{Sym}}(\mathrm{n_{FFT}} + \mathrm{n_{Prefix}})}\right)\mathrm{n_{Sub}} * \mathrm{Bits_{Sym}} \tag{3.28}$$

Where S represents the Sequence length, n_{FFT} is the number of FFT points, n_{Sub} is the number of subcarriers, and n_{Prefix} is the number of prefix points.

The BER expression for M-ary QAM is [5, 6]:

$$\begin{aligned} BER &= \frac{\sqrt{M}-1}{\sqrt{M}.\log_2\sqrt{M}}\operatorname{erfc}\left(\sqrt{\frac{3\log_2 M}{2(M-1)}\frac{\delta}{\sqrt{2}}}\right) \\ &= \frac{\sqrt{M}-1}{\sqrt{M}.\log_2\sqrt{M}}\operatorname{erfc}\left(\sqrt{\frac{3\log_2 M}{2(M-1)}\frac{\sqrt{2}B_0}{R_s}(OSNR)}\right) \end{aligned} \tag{3.29}$$

Where $\delta^{1/2}$ the known Q-factor is equals to $\frac{|\check{I}|^2}{\sigma_i^2}$

Where B_0 represents the optical ASE noise bandwidth used for OSNR measurements (typically 0.1nm), R_s is the symbol rate and σ_i is the total rms noise, without taking into account the noise that comes from background (sun radiation) and the ASE noises that occurs due to the amplifier stages. The σ_i expression that takes into consideration only the inherent detectors noises is given by the formula [7, 8-ch4]:

$$\sigma_i = \sqrt{\sigma_{th}^2 + \sigma_{dc}^2 + \sigma_{sn}^2} = \sqrt{\frac{4KTB_w}{R_L} + 2q_e I_d B_w + 2q_e R B_w P} \tag{3.30}$$

Where R represents the PIN responsivity, q_e is the electron charge, h is the Planck constant, B_w is the bandwidth of the detector filters, K is the Boltzmann constant, T represents the effective noise temperature, R_L represents the total effective input resistance of detectors, I_d is the overall dark current of the photo-detectors and P is considered as the total optical power that is detected through detection system.

3.4.2 BER analysis of QPSK

Using rectangular data pulse the power Spectral Density (PSD) of a QPSK signal is given by:

$$\begin{aligned} P_{QPSK} &= \frac{E_S}{2}\left[\left(\frac{\sin[\pi(f-f_c)T_S]}{\pi(f-f_c)T_S}\right)^2 + \left(\frac{\sin[\pi(f+f_c)T_S]}{\pi(f+f_c)T_S}\right)^2\right] \\ &= \frac{E_S}{2}\left[\operatorname{sinc}^2\big((f-f_2)T_S\big) + \operatorname{sinc}^2\big((f+f_2)T_S\big)\right] \end{aligned}$$

$$= \frac{E_S}{2}\left[\text{sinc}^2\left(\frac{(f - f_2)}{R_S}\right) + \text{sinc}^2\left(\frac{(f + f_2)}{R_S}\right)\right] \quad (3.31)$$

Where E_S represents energy per symbol, T_S is the symbol period, R_S is the symbol rate, and f_c is the carrier frequency.

The probability of bit error for QPSK is obtained as [15]:

$$P_b = Q\left(\sqrt{\frac{2E_b}{N_0}}\right) = \frac{1}{2}\text{erfc}\left(\sqrt{\frac{E_b}{N_0}}\right) \quad (3.32)$$

Where, Q(x) is the Q-function and the Q-factor can be evaluated from the equation 3.32:

$$Q^2 = 2\{\text{erfc}^{-1}(2 * \text{BER})\}^2 \quad (3.33)$$

CHAPTER FOUR

System Design, Simulation and Results Discussion

4.1 Introduction

This unit presents the simulation results of both CO- DP QPSK and CO-OFDM hybrid fiber/FSO systems. The systems are designed and simulated using OptiSystem tool and MATLAB software. Quadrature amplitude modulation (QAM) based OFDM and DP QPSK techniques are used into the systems separately. All the figures in this chapter are taken from MATLAB and OptiSystem tools.

4.2 OptiSystem Simulation Software

OptiSystem tool allows experts to design, test, and simulate optical links in the transmission layer of optical networks. Many optical fiber and FSO components are offered for designing and implementation of an optical network.

OptiSystem enables experts to design and simulate:

- Co-Simulation
- Advanced Modulation
- Access Networks
- Dispersion Management
- Multimode Systems
- Optical code division multiple access for Passive optical networks
- Fiber Analysis and Design
- Optical Amplifiers, receivers, transmitters

4.3 100Gbits/s CO-OFDM Hybrid System Design

Figure 4.1 shows the simulation design of a single channel CO-OFDM based hybrid optical fiber/FSO system.

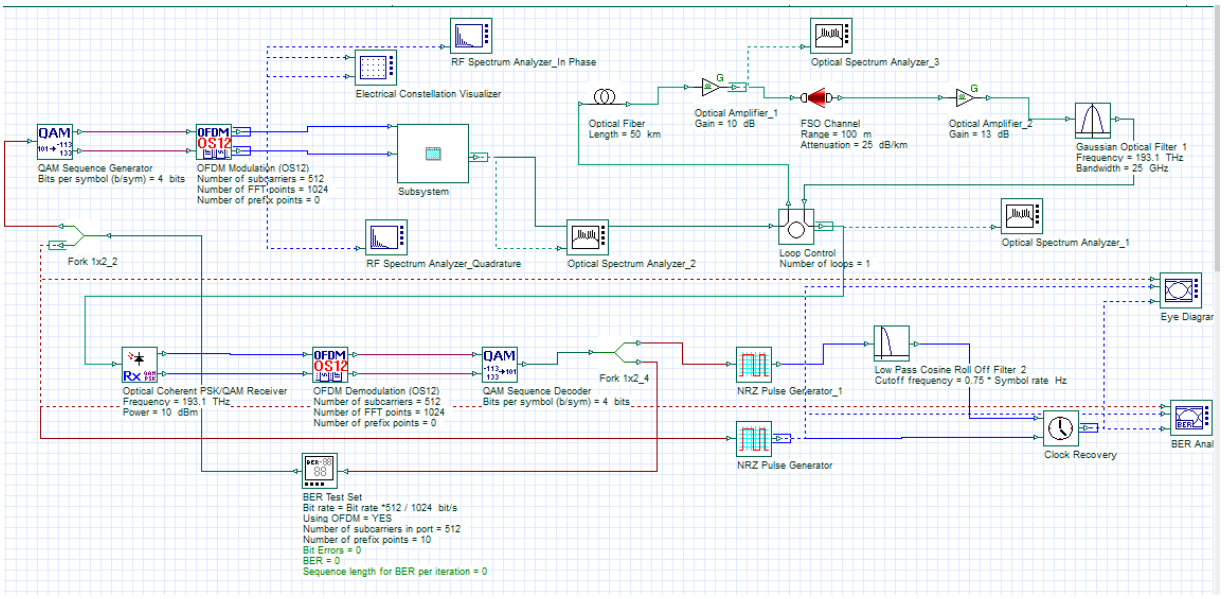

Figure 4 1: Block Diagram of CO-OFDM hybrid optical fiber/FSO System

4.3.1 QAM-OFDM system

In this thesis, a single channel hybrid optical fiber/FSO system is considered. For CO-OFDM hybrid system QAM modulation technique (16-QAM) is used for the generation and decoding of the digital signal. The 16-QAM modulator carries two digital bit streams by changing the amplitudes of two carrier signals, using the amplitude-shift keying (ASK) scheme. The two modulated signals are added, and the final waveform is a combination of both ASK and PSK.

In digital QAM scheme, a finite number of modulated signals at least two amplitudes and two phases are used. Figure 4.2 shows the constellation diagrams of 16-QAM.

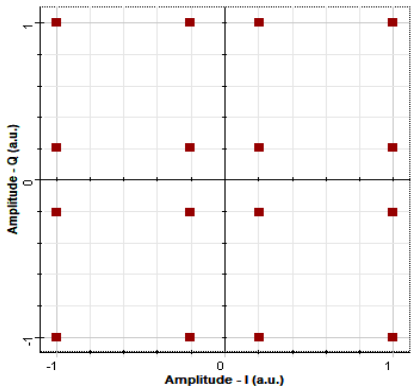

Figure 4 2: Constellation Diagram of 16-QAM

In Coherent optical OFDM system 512 sub-carriers and 1024 FFT points are used to get a BER value of zero.

1. Radio frequency transmitter

As shown in figure 4.3, the radio frequency transmitter is consists of a pseudo random binary sequence generator (PRBS), QAM sequence generator, OFDM modulator, and low pass filter components.

a. Pseudo random binary sequence (PRBS)

PRBS is the first block to generate a random bit sequence that will approximate the random data characteristics. For the CO-OFDM system, the simulation sequence length is assumed 131072 bits.

The output of PRBS is a deterministic and periodic signal with properties similar to white noise, and usually generated using an n-bit shift register with feedback through an exclusive or (XOR) function. Even if the PRBS signals appearing random, the sequence actually repeats every 2n–1 values.

b. QAM sequence generator

When the QAM sequence generator is used, the bit sequences are coded using gray coding which make ready for splitting into parallel sub-sets and each can be conveyed in two quadrature carriers when building a QAM modulator.

c. OFDM modulation

The serial output symbol streams of the QAM modulator is converted into a parallel format in the OFDM modulator. Then each parallel symbol is assigned to one carrier in the transmission.

After assigning the spectrum, inverse Fourier transform is used to find the corresponding time waveform and the gourd period (cyclic prefix) will be added to start each symbol.

After IFFT process the digital symbols are fed to DAC (step, linear, and cubic techniques) to output analog signal and the parallel data is converted back into the serial symbol stream.

In this thesis, the OFDM modulator has 512 subcarriers, 1024 IFFT points, and 10 prefix numbers.

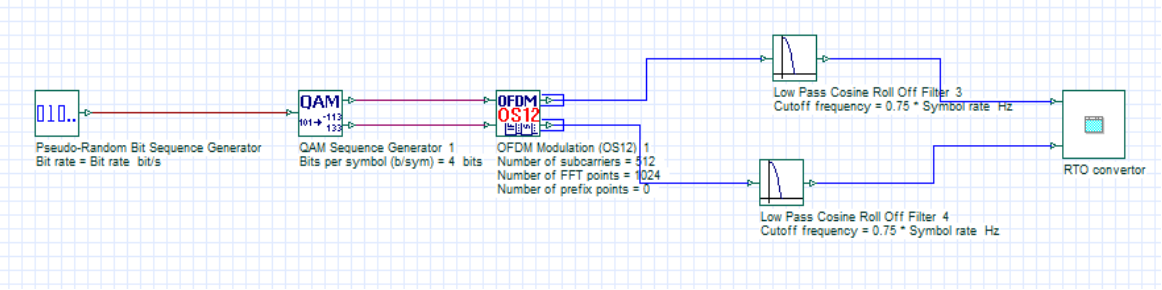

Figure 4 3: OFDM transmitter

2. Optical transmitter

The electrical to optical up conversion is done using the optical transmitter components and launches the resulting optical signal into the transmission medium. As shown in figure 4.4, the optical transmitter includes of an optical source, electrical pulse generator, and optical modulator.

External modulation is chosen to achieve chirp-free, high data rate, long-link length optical communication. As shown in figure 4.4, the optical modulator consists of two lithium Niobate (LiNbO3) Mach-Zehnder modulators (MZM). Lithium Niobate modulators or LN Modulators are characterized as high reliability, high data rate performance, stability over changing temperature conditions, good compatibility with optical fibers, low driving voltage, low drift in the transfer function, and multiple functions can be integrated into a single component.

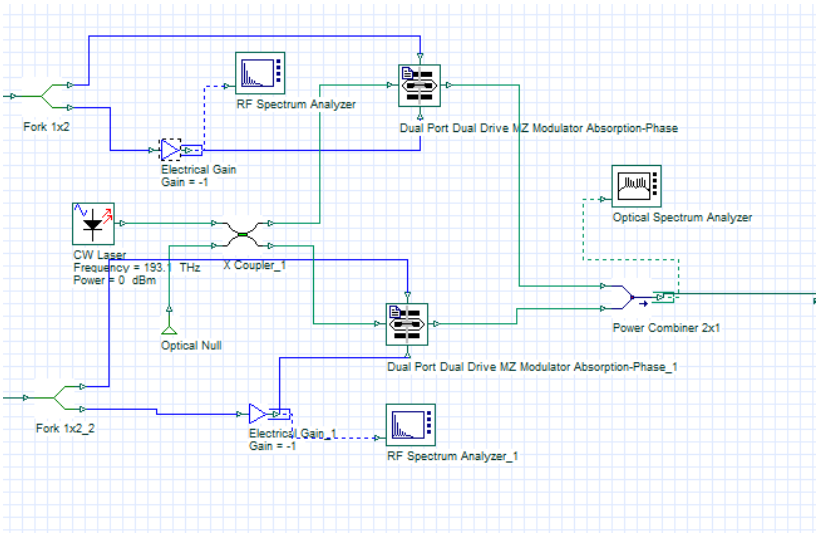

Figure 4 4: RTO convertor

Assuming no electro-optic effect, the modulator works when the biased electrodes are unbiased and separate switching voltages are applied to both electrodes, and the in phase waves add up at the 2nd junction giving a maximum output power.

4.3.2 The Optical transmission link

a) Optical fiber links

As shown in figure 4.5, the transmission link consists of an optical fiber with length of 50xN km distance. Hence, we have considered silica based fiber the attenuation is approximated to be 0.2dB/km and all other fiber parameters are chosen as: dispersion values of 16.75 and 30ps/ (km.nm), a dispersion slope of 0.075 (km.nm^2) and a nonlinearity coefficient 2.6×10^{-20}.

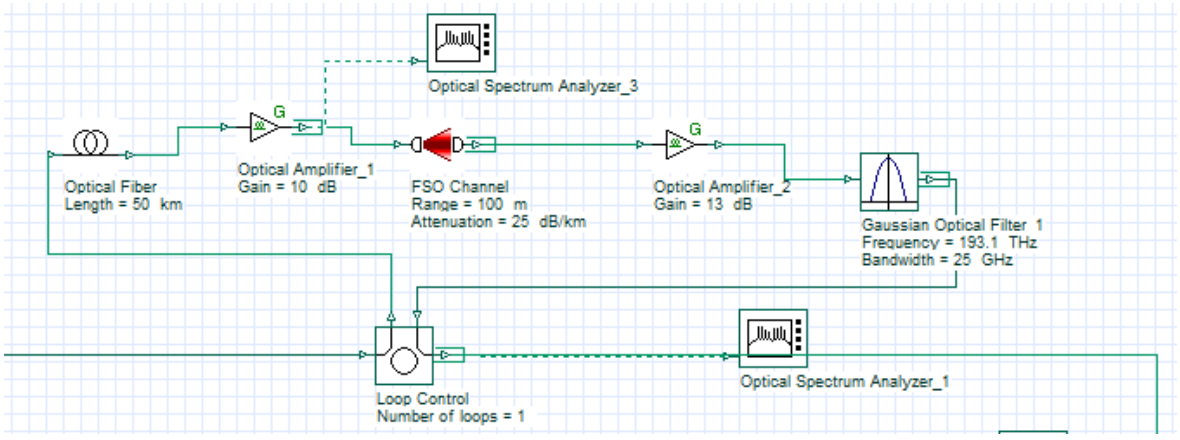

Figure 4 5: Fiber Link with 50 km SMF

b) FSO links

The FSO link is the subsystem of the transmission link consists of two telescopes and the free space channel between them. This component allows for simulation of free space optical links. The laser intensity power in depends the attenuation and Geometrical losses.

The attenuation loss describes the variation of the laser power in the atmosphere and geometrical loss occurs due to the spreading of the transmitted beam between the transmitter and the receiver. FSO system is best suited for the modeling of line of sight free space terrestrial links.

c) Amplifier gain and noise figure

An optical amplifier is required to amplify the weak signals for transmitting through a long distance fiber cable with the same window time to the CW laser. After receiving the rear end of the optical EDFA preamplifier, in addition to the noise outside the signal itself, but also the introduction of spontaneous emission (ASE) noise, and signal light ASE (S-ASE) on the detector and the noise generated by the ASE-ASE. In addition to the EDFA optical signal is amplified input signal but also noise signals for this same amplification EDFA gain is defined as:

$$G = (P_{out} - P_{ASE})/P_{in} \tag{4.1}$$

Where P_{in}, and P_{out} are the amplifier input and output signal power, and on behalf of EDFA P_{ASE} power output falls within the bandwidth of the signal light.

The noise figure can be calculated the ratio of input and output optical signal-to-noise ratio of the light, which reflects the degree of signal to noise ratio by the optical preamplifier after falling.

$$NF = 10 \log\left(\frac{SNR_{in}}{SNR_{out}}\right) \tag{4.2}$$

Using this formula can know the noise figure and gain influence by ASE noise, ASE noise greater NF bigger.

4.3.3 CO-OFDM receiver

The CO-OFDM receiver model consists of the optical and RF receiver components.

1) Optical receiver

Figure 4.5 shows the optical receiver or optical to RF down-converter (OTR). The optical signal comes from the optical modulator through a hybrid fiber/FSO links is detected by photo-detector. A band pass filter is used to eliminate the noise that added from fiber.

At the end of the link the optical signal is detected by photo-detector and the down conversion of optical to RF will be done to recover the original data. Assuming linearity in every stage of signal processing is maintained and ignoring the loss of the fiber and FSO junctions, the incoming signal and the radiation of the second laser diode are mixed together to form coherent detection. Each detector consists of two couplers and two PIN photo-detectors.

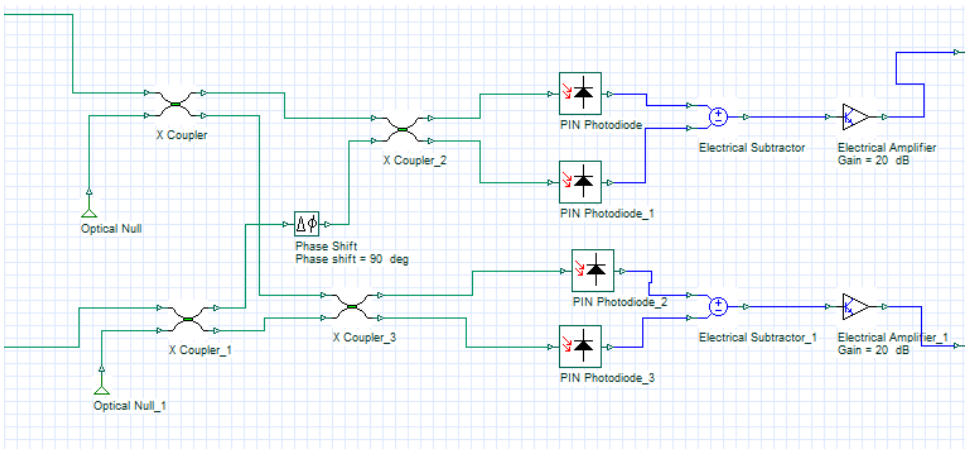

Figure 4 6: Coherent Detection

2) RF receiver

After the down conversion process, the signal will be demodulated with OFDM demodulator to extract the symbols and then decoded with 16QAM decoder to get the original bits. Figure 4.6 shows the RF receiver.

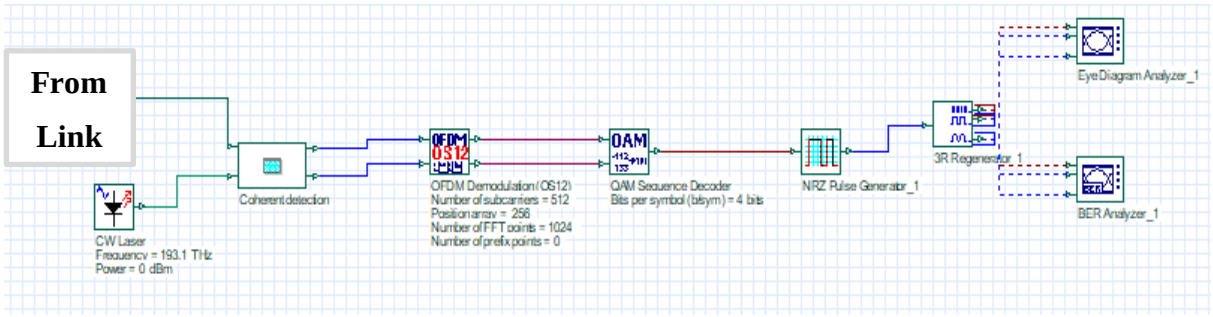

Figure 4 7: CO-OFDM Receiver

Table 4 1: SMF Parameters

Fiber Length	100-525 (km)
Attenuation	0.2 (dB/km)
Dispersion	16.75(ps/(km.nm))
Dispersion slope	0.075 (ps/(nm^2.km))
Effective area of the fiber core	80 (μm^2)
Nonlinear refractive index (n_2) of the core	2.6* 10^{-20}

4.3.4 Simulation results and discussion of a hybrid CO-OFDM system

Table 4.2 shows the global parameters setup for 100Gbits/s CO-OFDM system.

Table 4 2: Global Parameters Setup

Parameter	Value
Bit rate	100 Gbits/s
Time window	$6.5536 * 10^{-7}$ s
Sample rate	200 GHz
Sequence length	65536 bits
Sample per bit	2
Number of samples	131072

As shown in figure 4.7, the RF spectrum for the I/Q signals of the system at CO-OFDM transmitter with 41.89dBm power is measured. Figure 4.8 shows the optical signal spectrum, after modulating the electrical signal with the optical carrier using two MZMs while figure 4.9 illustrates the CO-OFDM spectrum after the propagation through the optical link.

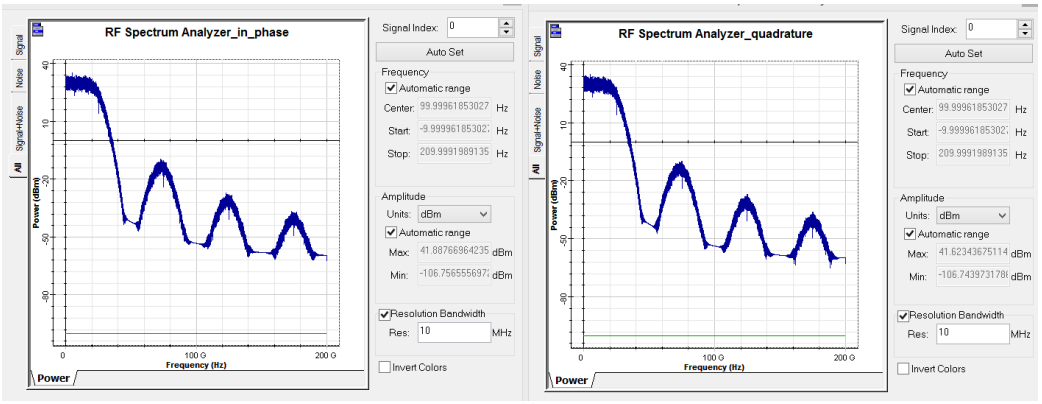

Figure 4 8: RF OFDM Spectrum I/Q of fiber part.

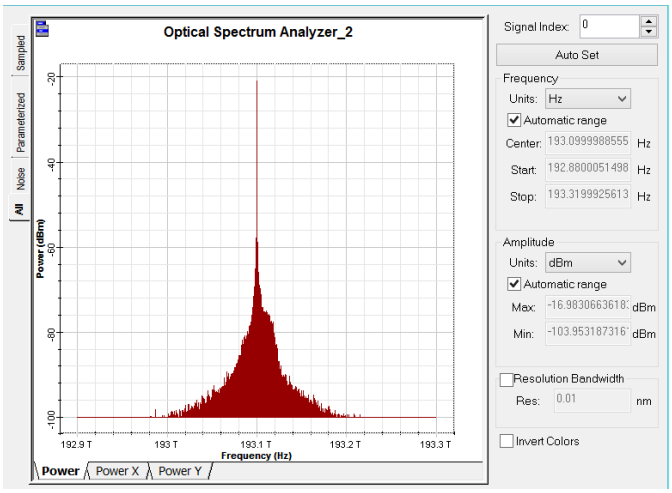

Figure 4 9: Optical OFDM spectrum after the two MZ modulators.

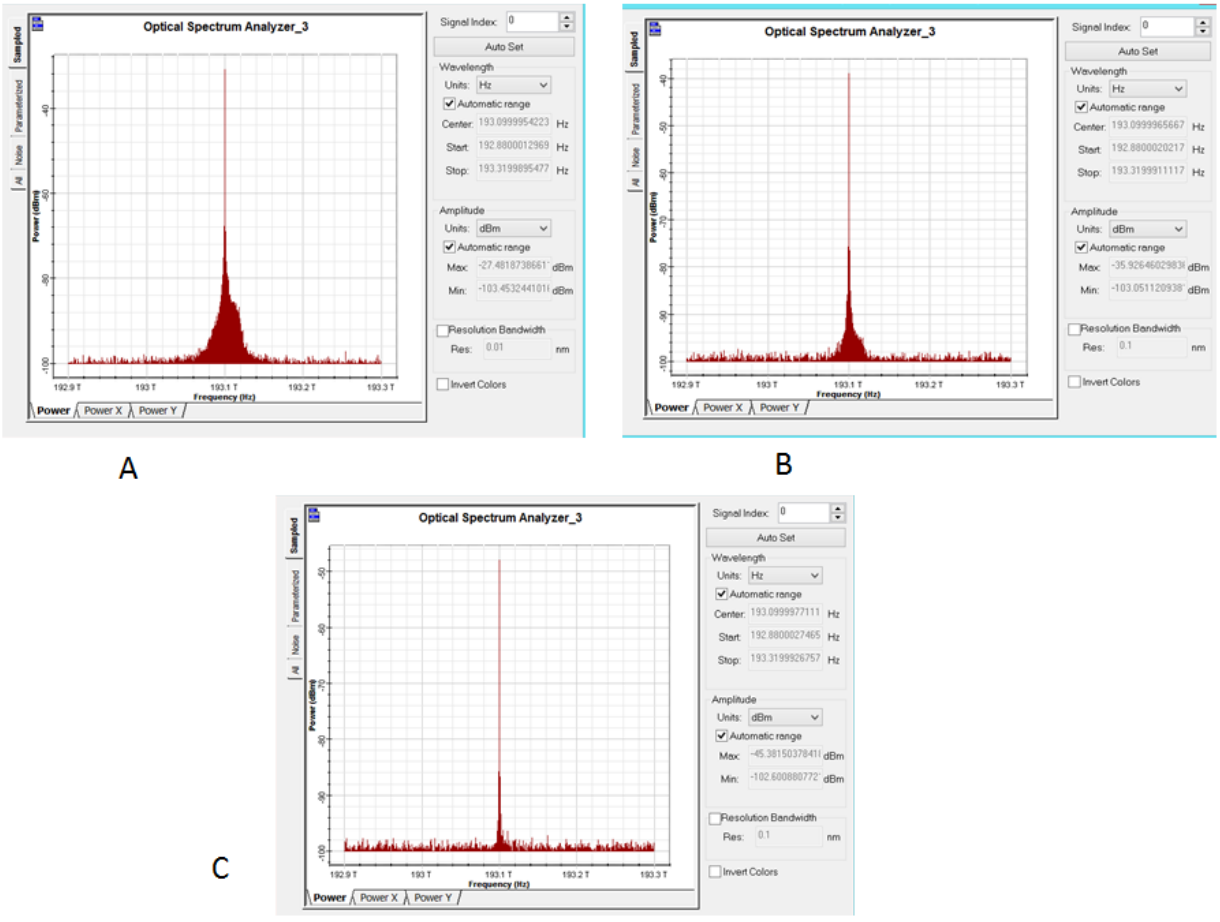

Figure 4 10: Coherent optical OFDM spectrum with dispersion (D) 16.75(ps/(nm.km)) after: A) 100km fiber link, B) 200km fiber link, and C) 300km fiber link.

As shown in figure 4.9 above, the optical OFDM signal after a hybrid 100km fiber at the CO-OFDM receiver side with a dispersion equal to 16.75(ps/(nm.km)) is measured a power about -27.482dBm. It is observed that as the fiber distance increases from 200km to 300km the optical power decreases from -35.926dBm to -45.38dBm.

Figure 4.10 shows a coherent optical OFDM spectrum with dispersion value of 16.75(ps/(nm.km)) and varying fiber links. After 100km fiber link the received power is measured at about -27.4832dBm. It is observed that as the fiber distance increases from 200km to 300km the optical power decreases from -37.98dBm to -48.485dBm.

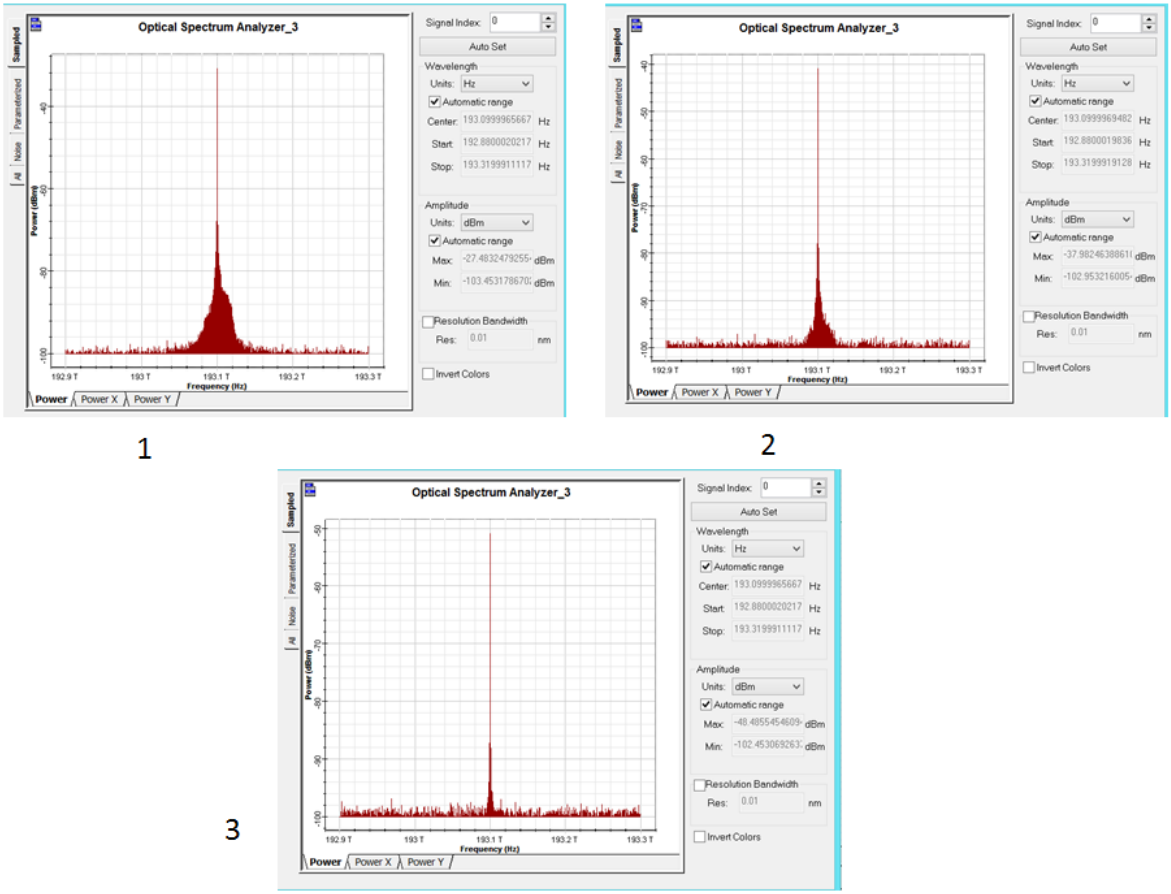

Figure 4 11: Coherent Optical OFDM spectrum with dispersion (D) 30(ps/(nm.km)) after: 1) 100km fiber link, 2) 200km fiber link, and 3) 300km fiber link.

Figure 4.11 shows the optical OFDM signal after the FSO link at the CO-OFDM receiver side and 100km SMF with a dispersion of 16.75(ps/(nm.km)).

At 200m FSO link the optical power is measured at about -34.876dBm. With the increasing of the FSO link from 400m to 600m the optical power decreased from -45.93dBm to -54.69dBm.

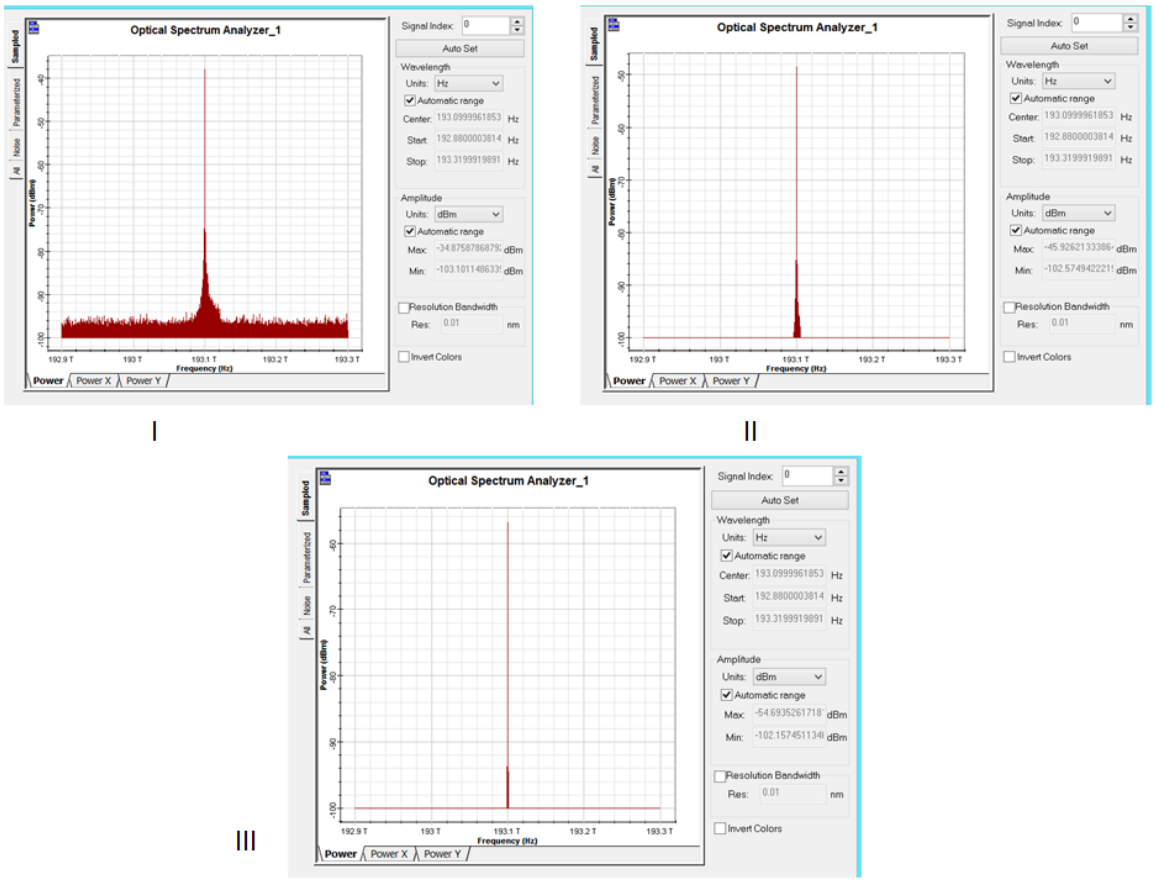

Figure 4 12: Coherent CO-OFDM spectrum after 100km fiber varying FSO links with 13dB EDFA gain; I) 200m FSO link, II) 400m FSO link, and III) 600m FSO link.

4.4 100Gbits/s CO-DP QPSK Hybrid System Design

Figure 4.12 shows the simulation design of a single channel CO-DP QPSK based hybrid optical fiber/FSO system.

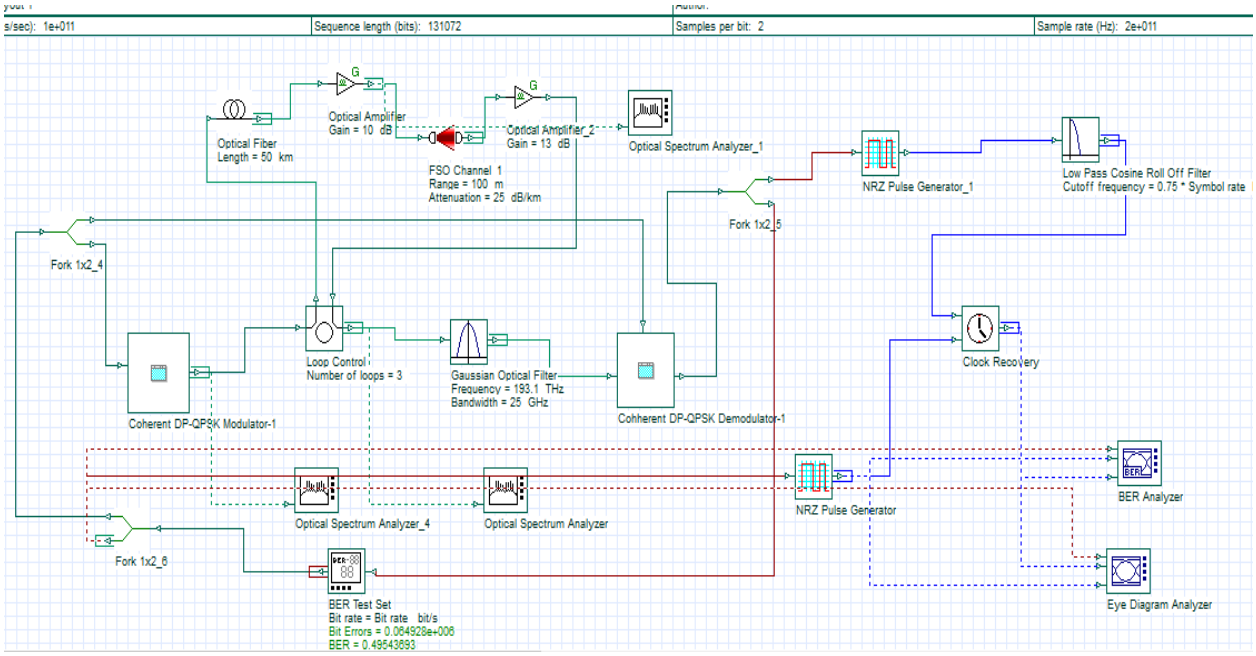

Figure 4 13: Block diagram of fiber/FSO optical DP QPSK system.

4.4.1 DP QPSK system

In this paper, a single channel hybrid optical fiber/FSO system is considered. The DP-QPSK consists of a polarization beam splitter, and two different QPSK data streams are modulated over the vertical and horizontal directions. It uses two orthogonal state of polarization (horizontal and vertical) of laser beam with I/Q modulator (QPSK) signal for digital modulation and encodes 4 bits/symbol rate. DP-QPSK is advantageous in optical communication to represent laser output into symbols for minimizing the BW of the transmission of information. The transmitted signal is encoded in both polarizations and phase. For 100 Gbits/s data rate the symbol rate 25 Gsymbol/s due to DP-QPSK modulation as it contains 4 bits/symbols in its constellation.

In DP-QPSK, the data bits to be modulated are grouped into symbols, each containing two bits, and each symbol can take on one of four possible values: 00, 01, 10, or 11. During each symbol interval, the modulator shifts the carrier to one of four possible phases corresponding to the four possible values of the input symbol.

In the ideal case, the phases are each 90 degrees apart, and these phases are usually selected such that the signal constellation matches the configuration shown in figure 4.13.

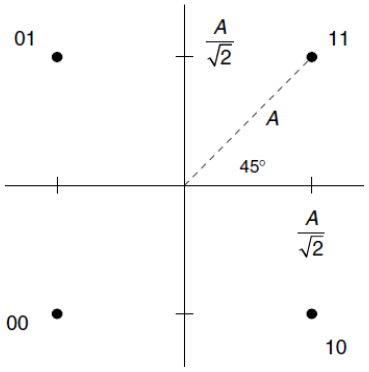

Figure 4 14: QPSK constellation.

When I and Q take on values of $\frac{\pm A}{\sqrt{2}}$ in all possible combinations, the phase of the resulting output signal takes on values of 45, 135, 225, and 315 degrees.

The optical CO-DP-QPSK system consists of five main parts: DP-QPSK transmitter, transmission link, coherent receiver, digital signal processing, and detection & decoding (which is followed by direct-error-counting).

4.4.2 DP QPSK transmitter

As shown in figure 4.14, the DP QPSK transmitter is consists of two blocks.

1) Radio frequency transmitter

And also the radio frequency transmitter is consisted of two blocks.

The first block is a PRBS to generate a bit sequence that will approximate the random data characteristics. In this simulation the sequence of length is 131072 bits.

The second block is two QPSK (4 bit per symbol) modules to generate bits per symbol. Each QPSK modulator uses 2 PSK (each 2 bit per symbol) sequence generators to convert the random bits to PSK signal form and pass to M-ary pulse generator.

The modulator output sent to an electrical amplifier which has a power gain greater than one and electrical bias in order to establish proper operating conditions for the component.

2) Optical transmitter

RF to optical up conversion (RTO) is done using the optical transmitter components and launches the resulting optical signal into the optical fiber. The optical transmitter includes an optical source with splitter, electrical pulse generator and optical modulator which consists of two lithium Niobate (LiNbO3) Mach-Zehnder modulators (MZM).as shown in figure 5.19.

Polarization beam splitter (PBS) are important components for various optical information processing applications such as optical switching networks, read-write magneto-optic data storage systems, and polarization based imaging systems. The light intensity consists of two orthogonally polarized components traveling along the same path and can be separated with a polarizing beam splitter into distinguishable spatial paths. In general, there is no conceptual difference between the field before and after this transformation.

The output beam from the splitter is dependent on both the transmission and reflection index. If a linearly polarized infrared beam, with, then the beam is

To split the beam into two orthogonally polarized beams, consider a linearly polarized beam with a direction of polarization at 45 degrees relative to the polarization direction of the beam-splitter. In this paper, the device angle for both splitter and combiner is considered 45^0.

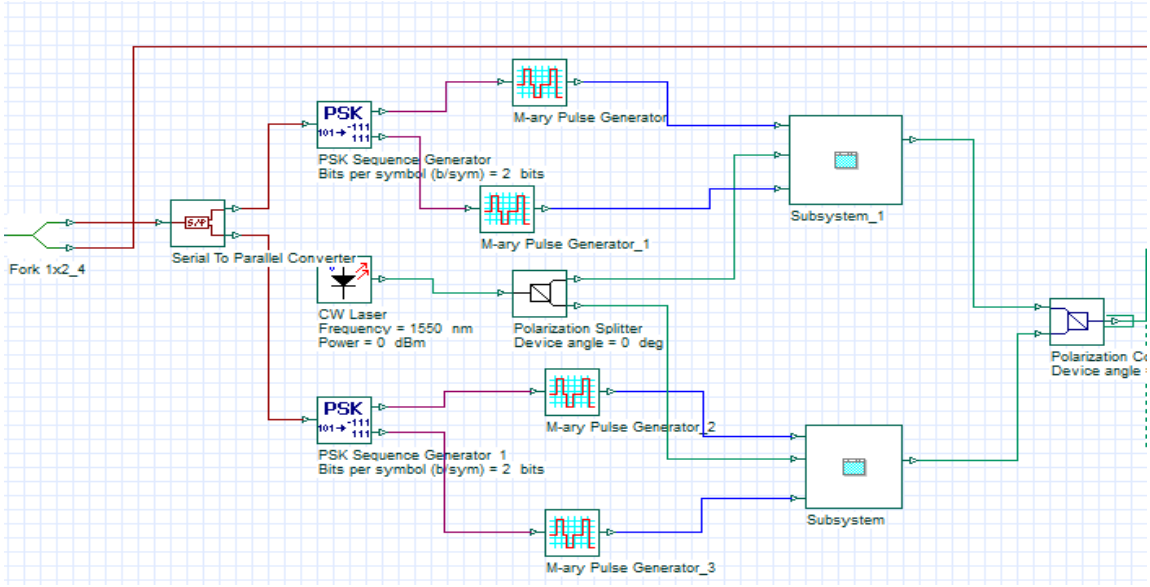

Figure 4 15: DP QPSK transmitter

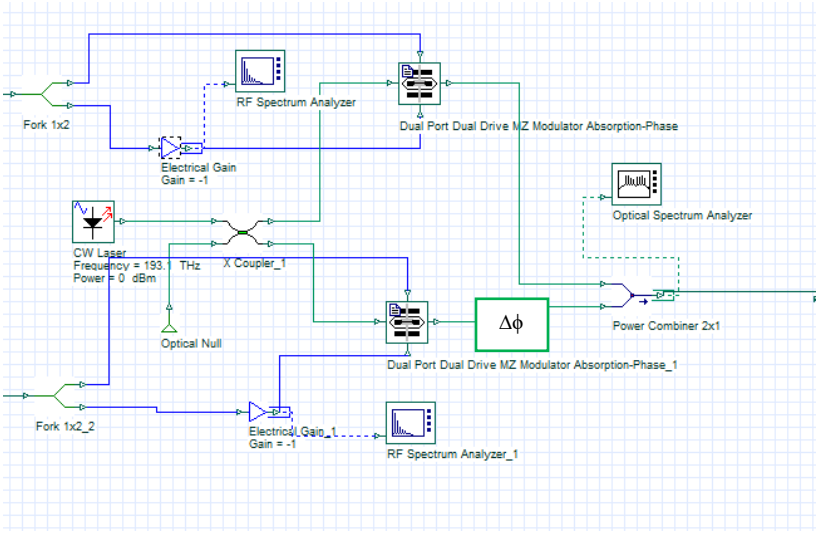

Figure 4 16: Electrical to Optical Convertor subsystem.

4.4.3 Optical transmission links

Similarly, as shown in figure 4.5 the transmission link consists of an optical fiber with length of 50xN km and FSO link with 100xN distance. Hence, we have considered silica based fiber the attenuation is approximated to be 0.2dB/km and all other fiber parameters are chosen as: dispersion values of 16.75 and 30ps/(km.nm), a dispersion slope of 0.075 and 0.1343ps/(km.nm^2) and a nonlinearity coefficient 2.6×10^{-20}. An optical amplifier is used to amplify the weak signals with the same window of the laser diode.$\Delta\emptyset$

4.4.4 Coherent detection and receiver

The coherent detector is required to sense the modulated optical DP-QPSK signal. The receiver section consists of a polarization beam splitter, a laser diode, phase shifter, balanced photo detectors, electrical subtractors, electrical amplifiers, threshold detector, PSK decoder, and serial to parallel converter. By combining all components, the amplitude and phase of the transmitted signal can be recovered. After down conversion, the amplified signal passed to DSP which equalizes the linear transmission impairments such as group velocity dispersion (GVD) and PMD of optical fiber. The threshold detector/decision processes the I/Q electrical signals received from DSP stages and normalize the electrical amplitudes of each I and Q channels to respective M-ARY grids to perform decision for each received symbols into threshold levels.

Finally, the signal is decoded into binary signals and pass into parallel to serial converter to produce DP-QPSK signal at output and then to the BER Test Set for direct-error-counting.

1. Coherent DP-QPSK detection

At the end of the hybrid optical fiber/FSO link the transmitted light intensity is detected and due to the down conversion procedures, the data are recovered. Assuming linearity in every stage of signal processing is maintained and ignoring the loss of the fiber and FSO junctions, the incoming signal and the radiation of the second laser diode are mixed together to form coherent detection. Each detector consists of two couplers and two PIN photo-detectors.

2. DSP

The coherent DP-QPSK detection technique is gained popularity on advancement of digital signal processing (DSP). DSP can improve the performance of a coherent receiver by implementing different algorithms, such as frequency offset and carrier phase estimations (FOE & CPE), digital backward propagation (DBP), and constant modulus algorithm (CMA), for the purpose of compensating phase noise and transmission impairments caused by frequency offset, line-width, chromatic dispersion (CD), nonlinear and polarization mode dispersion (PMD). After processing, the signal is sent to polarization decision maker which is dual polarized. Finally, the resulting signal is sent into a PSK decoder to recover the original binary signal as shown in the figure 4.12.

Table 4 3: Optical Fiber & FSO parameters

Parameters	SMF	FSO
Length	100-600km	< 1km
Attenuations	0.2dB/km	25 dB/km
Dispersion	16.75, 30ps/nm/km	NIL
Effective area	80 μm^2	NIL
EDFA gain	10, 13dB	NIL
EDFA noise figure	4dB	NIL
Distance	50km × N span	NIL
Beam Divergence	NIL	0.25mrad
Aperture Diameter	NIL	T=5cm, R=7.5cm

Table 4 4: Component parameters

Parameters	Value
CW laser frequency	193.1GHz
CW laser power	-5dBm
Switching voltage	4V
Modulation voltage	2V
Optical ASE noise BW	0.1nm
PIN responsivity	1A/W
PIN BW	2GHz
PIN dark current	10nA
Effective noise temperature	298K

4.4.5 Simulation results and discussion of CO-DP QPSK system

The simulation results of a hybrid optical fiber/FSO with CO- DP-QPSK are presented and discussed in this section.

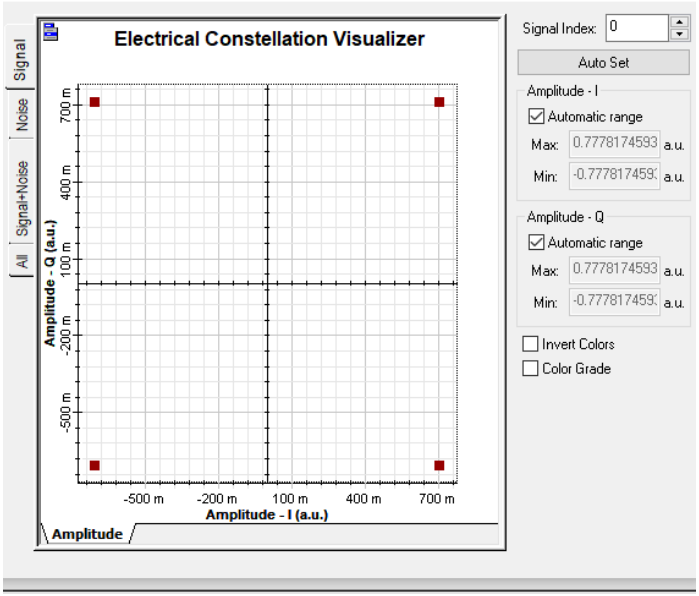

Figure 4 17: Constellation Diagram of QPSK

Figure 4.17 shows the RF spectrum for the I/Q signals of the system at CO-DP QPSK transmitter with at almost 20.08dBm RF power. Figure 4.18 shows the optical signal spectrum after modulating the electrical signal with the optical carrier using two MZMs.

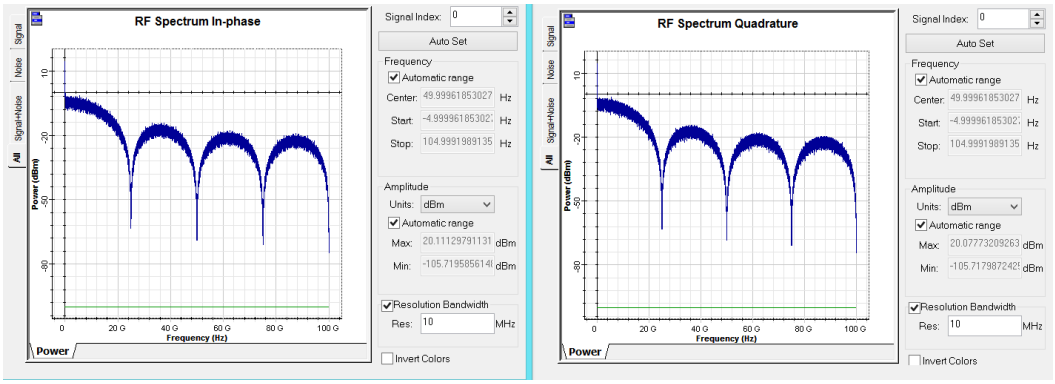

Figure 4 18: RF DP-QPSK Spectrum I/Q.

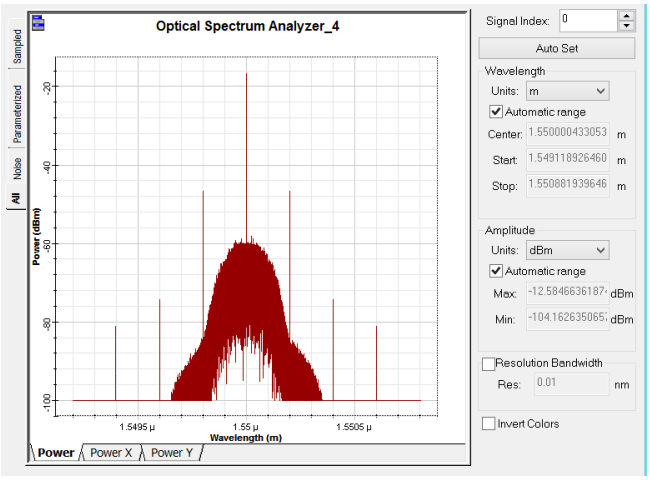

Figure 4 19: Optical DP-QPSK Spectrum after the two MZ Modulators for fiber transmission.

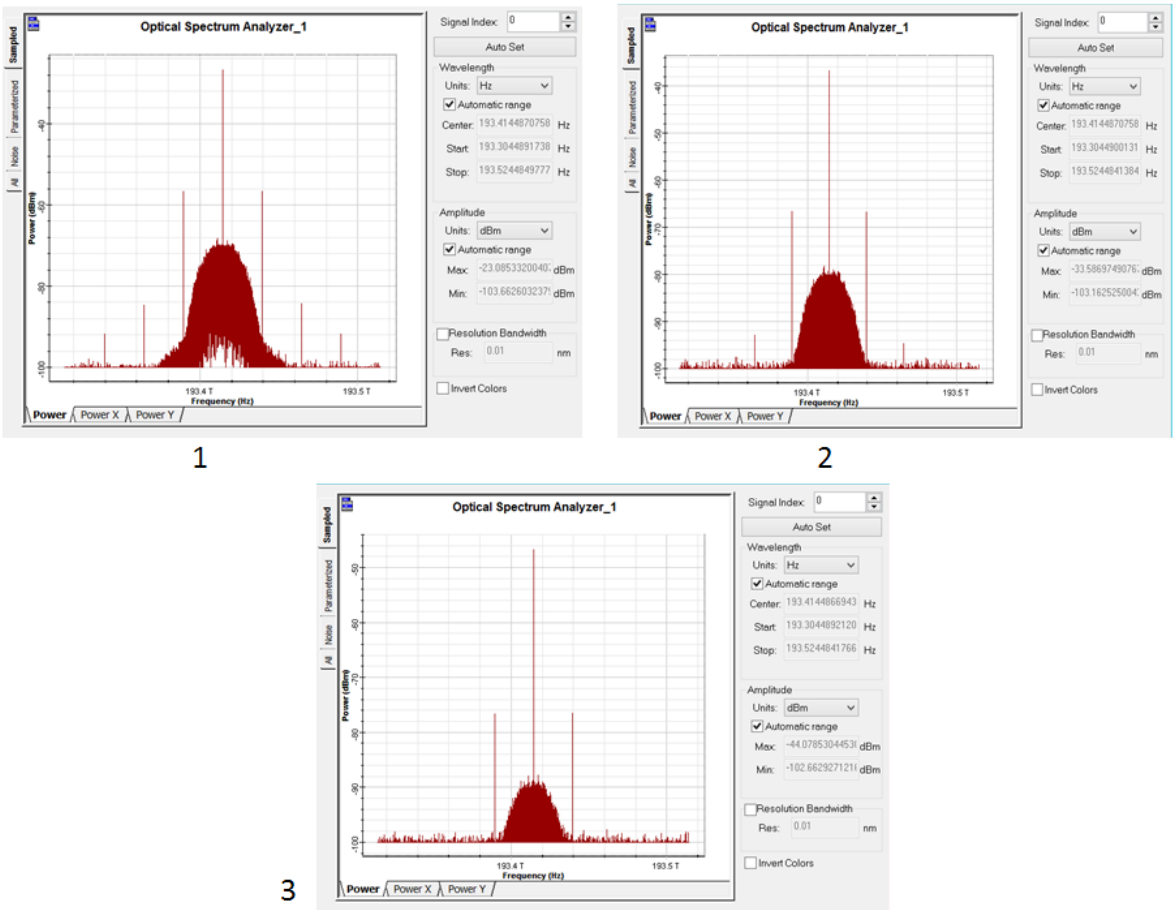

Figure 4 20: Coherent optical DP-QPSK spectrum with dispersion (D) 16.75(ps/(nm.km)) after: 1) 100km fiber link, 2) 200km fiber link, and 3) 300km fiber link.

Figure 4.19 above shows a coherent optical DP-QPSK spectrum with dispersion value of 16.75(ps/(nm.km)) and varying fiber links. After 100km fiber link the received power is measured at about -23.0853dBm. It is observed that as the fiber distance increases from 200km to 300km the optical power decreases from -37.58694dBm to -44.07853dBm.

As shown in figure 4.20, the optical QP-QPSK signal spectrum after 100km fiber at the CO-DP QPSK receiver side with a dispersion equal to 30(ps/(nm.km)) is measured a power about -23.0855dBm. It is observed that as the fiber distance increases from 200km to 300km the optical power decreases from -33.58697dBm to -44.07855dBm.

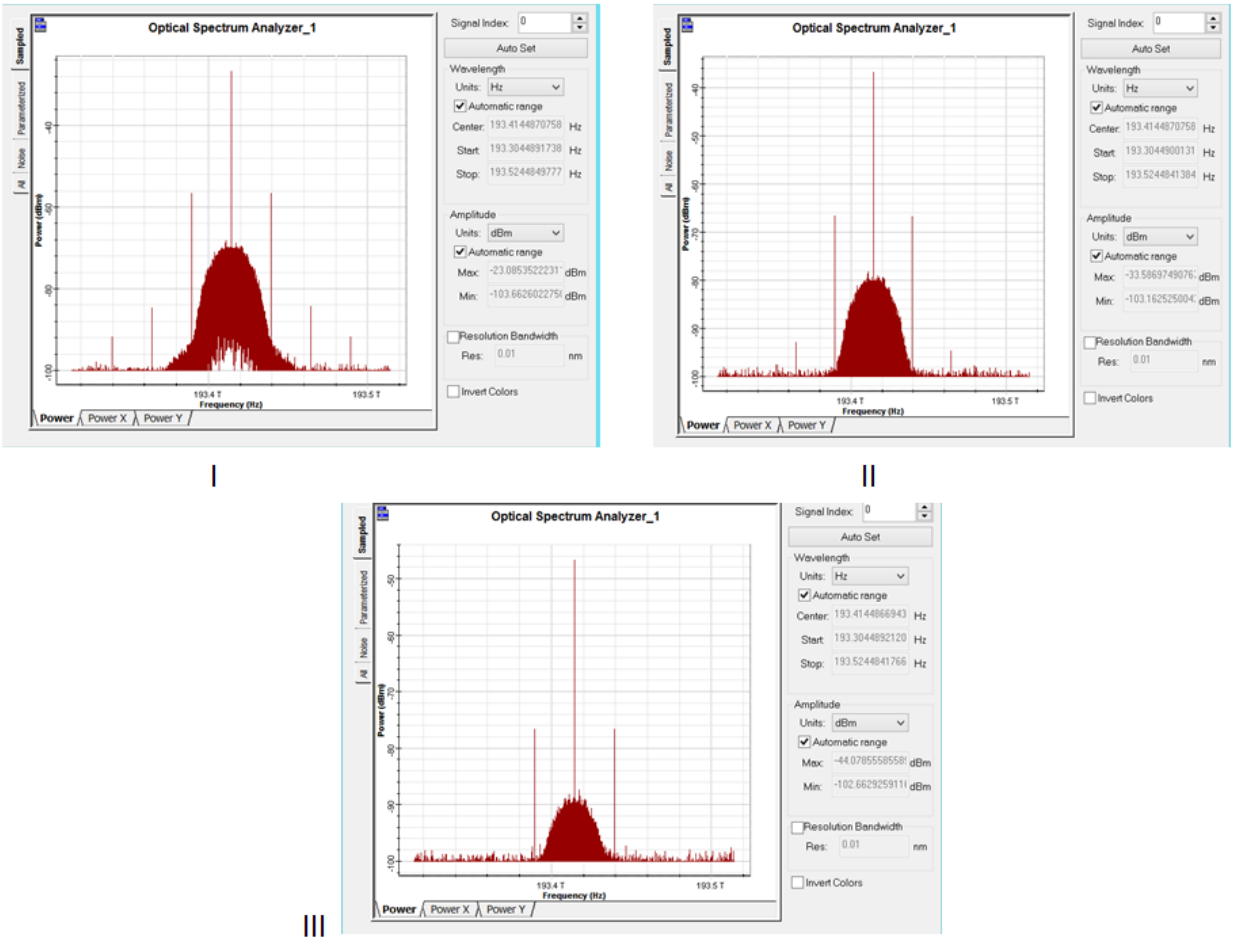

Figure 4 21: Coherent optical DP-QPSK spectrum with dispersion (D) 30(ps/(nm.km)) after: I) 100km fiber link, II) 200km fiber link, and III) 300km fiber link.

Finally, the output of the fiber link is amplified with 13dB gain for FSO link transmission. Figure 4.21 shows the optical DP-QPSK signal after the FSO link at the CO-DP QPSK receiver side and 100km SMF with a dispersion of 16.75(ps/(nm.km)). At 200m FSO link the optical power is measured at about -30.482dBm. With the increasing of the FSO link from 400m to 600m the optical power decreased from -41.53dBm to -50.299dBm.

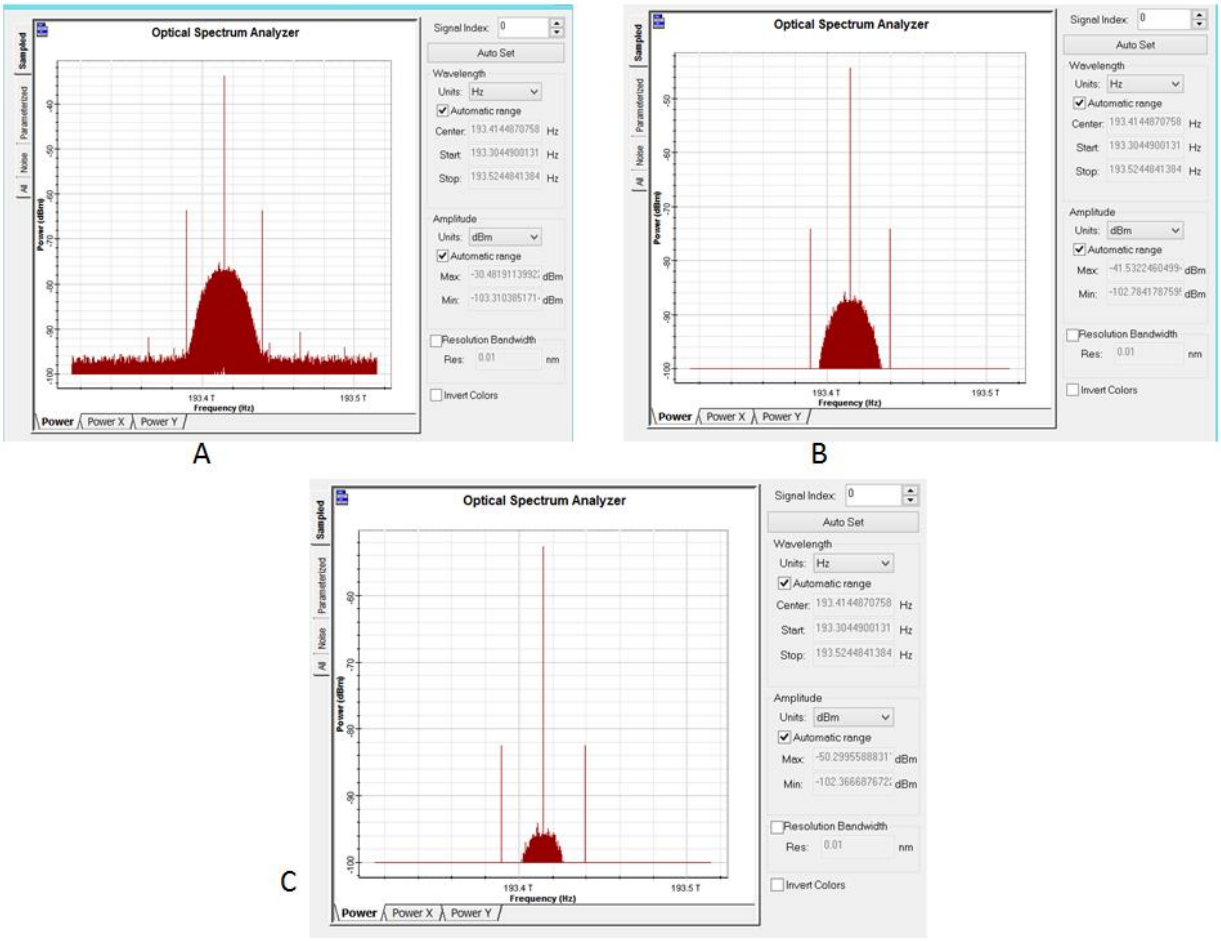

Figure 4 22: Coherent CO-DP QPSK spectrum after 100km fiber varying FSO links with 13dB EDFA gain; A) 200m FSO link, B) 400m FSO link, and C) 600m FSO link.

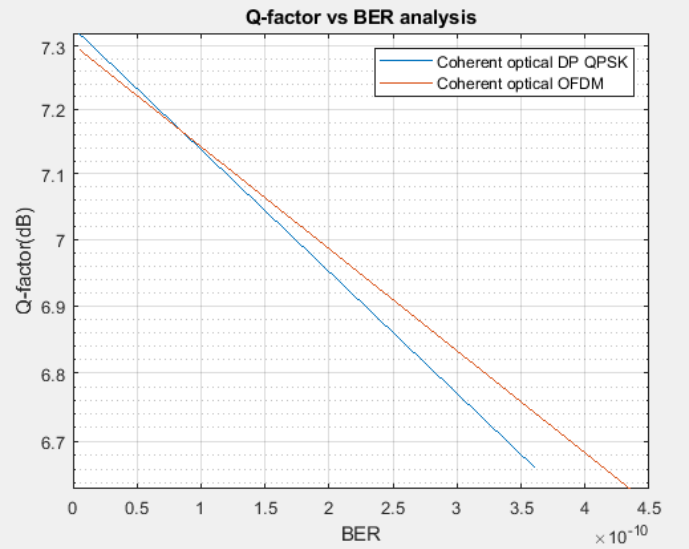

Figure 4 23: Q-factor versus BER analysis

As shown above in figure 4.23, when the hybrid link range increases the signal power reduced due to the attenuation and dispersion for the CO-DP QPSK system than the hybrid CO-OFDM system which limits the maximum achievable optical signal to noise ratio (OSNR) and quality factor. But, the narrow bandwidth nature of QPSK with lower attenuation and dispersion can achieve higher OSNR for short link range.

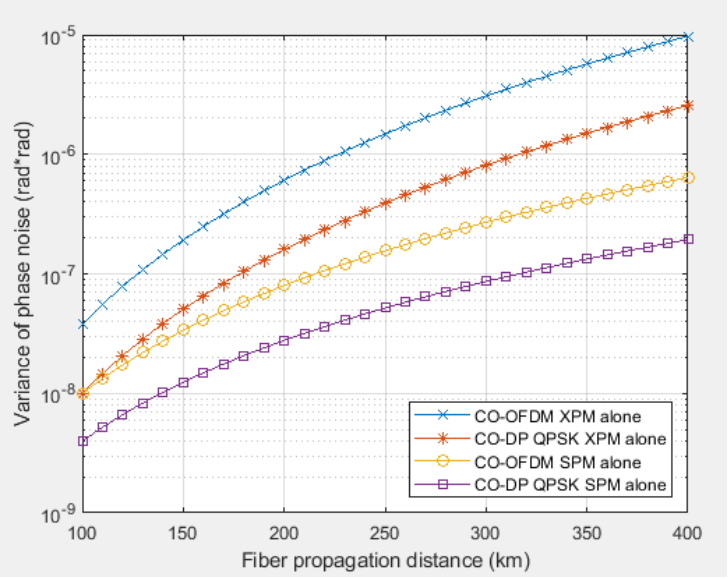

Figure 4 24: Non-linear variance of phase noise for CO-DP QPSK and CO-OFDM hybrid systems.

As shown in figure 4.24, the variance of nonlinear phase noise caused by the interaction of amplified spontaneous emission (ASE) noise with fiber nonlinearity such as self-phase modulation (SPM) and cross-phase modulation (XPM) is estimated in both hybrid systems.

Due to its multicarrier nature, dispersion tolerance (D) and high peak to average power the CO-OFDM system has higher nonlinear phase shift than the CO-DP QPSK system. As nonlinear effects are strongly dependent of the optical power and dispersion values during propagation, a usual method to avoid it is to keep low signal power during transmission, and then considering a linear propagation model. However, limiting the signal power also limits the maximum achievable Optical Signal-to-Noise Ratio (OSNR), penalizing system performance and in figure 4.25 the CO-OFDM system has higher average received power than CO-DP QPSK system at the same fiber length. This implies that the CO-OFDM signal can transmit more fiber length with nonlinearity drawbacks.

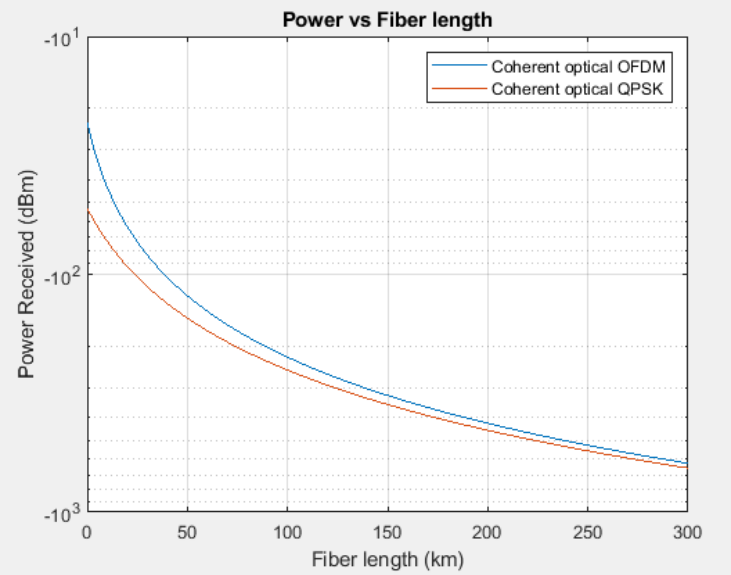

Figure 4 25: The optical received power versus fiber length for both CO-DP QPSK and CO-OFDM hybrid systems.

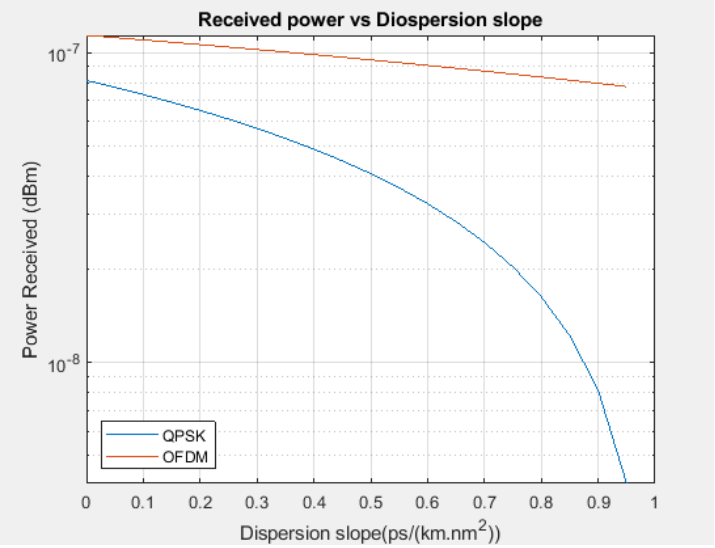

Figure 4 26: The optical received power versus dispersion slope for both CO-DP QPSK and CO-OFDM hybrid systems.

As shown in figure 4.26, the CO-OFDM system has good performance of the received power against dispersion that determined by the length of cyclic extension (CE). When the dispersion value increase the received power will decrease for both CO-OFDM and CO-DP QPSK fiber/FSO hybrid systems. As a result the CO- OFDM system can maintain the signal power even the dispersion value increases whereas the CO- DP QPSK system cannot tolerate if the dispersion increases which requires compensation techniques.

CHAPTER FIVE

Conclusion and Future Works

5.1 Conclusion

This paper presents an optical communication system with hybrid optical fiber/FSO links using advanced DP-QPSK and OFDM modulation techniques for coherent optical access downlink system to provide flexible user access with high bandwidth efficiency.

Free space optical links are more sensitive to atmospheric turbulence which induces channel fading and path loss resulting limitations of coverage areas. While, optical fiber technologies also induce dispersion and non-linearity effects which require compensation technique.

A hybrid optical fiber/FSO communication link is applied to minimize the separate fiber link and FSO link high data transmission drawbacks which give complementary option one to another and mitigate the drawbacks. OFDM and DP-QPSK advanced modulation techniques are applied to reduce the transmission restrictions and transmit higher data rate signals at a time per single channel.

In this thesis, two systems were modeled for 100Gbps data rate using coherent OFDM and DP-QPSK modulation techniques. The presented hybrid optical fiber/FSO system consists of a FSO link and Fiber link set up. The links are designed, simulated and analyzed using MATLAB software and OptiSystem tool.

The first system is a CO-OFDM hybrid link, 100Gbps data rate and 16-QAM modulation type, with 512 maximum numbers of subcarriers and 1024 FFT points. The designed and simulated system achieves best BER values up to 220km fiber and 510m FSO links.

The second system is CO-DP QPSK with a hybrid SMF/FSO transmission link; data rate was 100Gbps with 4-PSK modulation type. The designed and simulated system achieves the best BER values up to 202km fiber and 468m FSO.

It is observed that, having different dispersion values the power received on CO-OFDM system have lower rate than the DP-QPSK system. And also, CO-OFDM system has high tolerance against linear signal distortion effects and sensitive to nonlinear effects specially the XPM and four-wave-modulation (FWM) which affects the system performance.

5.2 Future Works

1. Optoelectronic integrated circuits for coherent optical OFDM/DP-QPSK

Optoelectronic integrated circuits (OEICs) will reduce the deployment of large number of optoelectronic devices and replace onto a single chip.

The main reasons for the use of OEICs are:

- ✓ It can support software: Through electronic signal processing, the photonic chip can be reconfigured for multiple functionalities in a number of aspects of transmission, reception, and filtering.
- ✓ It can provide enhanced performance: Improvement of the speed and noise performance can be achieved by integration due to the reduction of parasitic reactance, an almost perfect matching condition for balanced devices and mechanical stability.

2. WDM based fiber/FSO system with OFDM/DP-QPSK

Wavelength Division Multiplexing (WDM) based systems can improve a transmission system with a high bandwidth, a significant data rates, and a high spectral efficiency without increasing the cost or the complexity of the system. WDM based CO-OFDM/DP-QPSK systems have been proposed as a solution for the increased demand in bandwidth and the data rates.

References

[1] A. Malik, P. Singh, “Free Space Optics: Current Applications and Future Challenges”, International Journal of Optics. 2015 (2015) 1-7. doi:10.1155/2015/945483.

[2] D. Maharana (M-tech Scholar), Mrs. Ranjita Rout (Assistant Professor) , “A 4 channel WDM Based Hybrid Optical Fiber/FSO Communication System using DP QPSK Modulation for Bit Rate of 100/112 Gb/s”, IJER, ISSN: 2278-0181,Vol. 8 Issue 06, 2019.

[3] H. Ali , “Modeling and Simulation of High Speed Optical Fiber Communication System with OFDM”, ASRJETS, 2017.

[4] C. P. Gage, “Towards a Modular, Low-Power, Low-Cost, and High-Speed Underwater Optical-Wireless Communication Transmitter”, University of California San Diego, 2019.

[5] M. Zhu, “High-Capacity Communication Systems Using Advanced Optical And Wireless Technologies”, Georgia Institute of Technology,May, 2015.

[6] R. Lin, “High-Capacity Short-Reach Optical Communications”, KTH Royal Institute of Technology School of Information and Communication Technology”, SE-164 40 Kista, SWEDEN, December 2016.

[7] S. patnaik, S. sahu, A. Panda, C. Jaiswal, “Free Space Optical Communication: a review”, International Research Journal of Engineering and Technology. 03 (2016).

[8] Q. Yang, “High-speed Coherent Optical Orthogonal Frequency Division Multiplexing Design and Implementation”, the University of Melbourne, Australia, 2010.

[9] A. Malik, P. Singh, “Free Space Optics: Current Applications and Future Challenges”, International Journal of Optics. 2015 (2015) 1-7. doi:10.1155/2015/945483.

[10] L. Tao, Y. Ji, J. Liu, A. P. T. Lau, N. Chi, and C. Lu, “Advanced modulation formats for short reach optical communication systems”,IEEE Netw., vol. 27, no. 6, pp. 6-13, 2013.

[11] L. Li, W. Jian-yi, Z. Xiu-tai, and L. Hong-an, “Research on Mixed Data Rate and Format Transmission in WDM Networks”, vol. 11, no. 1, 2013.

[12] L. Tao, Y. Ji, J. Liu, A. P. T. Lau, N. Chi, and C. Lu, “Advanced modulation formats for short reach optical communication systems”,IEEE Netw., vol. 27, no. 6, pp. 6-13, 2013.

[13] Y. Feng, Z. Teng, F. Meng, and B. Qian, **“**An Accurate Modulation Recognition Method of QPSK Signal”, School of Information Science and Engineering, Shenyang Ligong University, Shenyang 110159, China, 19 May 2015.

[14] B. Mikkelsen; C. Rasmussen; P. Mamyshev; F. Liu,“Partial DPSK with excellent filter tolerance and OSNR sensitivity”, Electron. Lett. 2006, 42, 1363-1364. [CrossRef].

[15] Y. Chen,“A wideband photonic microwave phase shifter with 360-degree phase tunable range based on a DP-QPSK modulator," Opt. Commun. 2018, 410, 787-792. [CrossRef]

[16] H. Yin , Y. Yu and Z. Huang, “DLI-Based DP-QPSK Reception Scheme for Short-Range Optical Communication”, College of Intelligent Science and Technology, National University of Defense Technology, 13 July 2020.

[17] Y. Chen; A.Wen; Y. Wu,“Photonic generation of binary and quaternary phase-coded microwave waveforms with an ultra-wide frequency tunable range,” Opt. Express 2014, 22, 15618–15625. [CrossRef] [PubMed]

[18] F.; Gonthier, F. Tuneable, “all-fiber, delay-line interferometer for DPSK demodulation”, In Proceedings of the Optical Fiber Communication Conference 2005, Anaheim, CA, USA, 6-11 March 2005.

[19] B. U. Rindhe, J. Digge, and S. K. Narayankhedkar, “Implementation of optical OFDM based system for optical networks,” 2014 Int. Conf. Adv. Commun. Comput. Technol. (ICACACT 2014), vol. 4, no. Cd, pp. 1-9, 2014.

[20] J. Armstrong, “OFDM for Optical Communications”, J. Lightwave Technol. 2009, 27, 189-204.

[21] M, Ahmed, D. Al-Taae, “OFDM Performance in Multi-Mode Optical Fiber compared with conventional BPSK and QAM modulation”, Arts, Sciences& Technology University in Lebanon, 2015.

[22] Y. Tang, “High-speed Optical Transmission System Using Coherent Optical Orthogonal Frequency-Division Multiplexing”, University of Melbourne Australia, 2010.

[23] K. Alatawi, “high data rate coherent optical OFDM system for long-haul transmission”, SECS, University of Denver, 2013.

[24] L. Hanzo, S. X. Ng, T. Keller, and W. Webb, "Quadrature amplitude modulation: From basics to adaptive trellis-coded, turbo-equalized and space-time coded OFDM, CDMA and MGCDMA systems", John Wiley and Sons, New York, 2004.

[25] J. Tang, P. Lane, and K. Shore, “High-speed transmission of adaptively modulated optical OFDM signals over multimode fibers using directly modulated DFBs,” Journal of Lightwave Technology, 2006.

[26] N. Veneetha, K. Joseph, and R. Asha, “Performance analysis of direct detection and coherent detection system for optical OFDM using QAM and DPSK,” IOSR Journal of Engineering, Vol.7, no.7, July, 2013.

[27] M.Z. Chowdhury, M.T. Hossan, A. Islam, Y.-M. Jang, “A comparative survey of optical wireless technologies: architectures and applications”, IEEE Access 6 (Jan. 2018) 9819-9840.

[28] W. Shieh; C. Athaudage, "Coherent optical orthogonal frequency division multiplexing," Electronics Letters , vol.42, no.10, pp. 587-589, 11 May 2006.

[29] W. Shieh, X. Yi, and Y. Tang, “Transmission experiment of multi-gigabit coherent optical OFDM systems over 1000 km SSMF fiber,” Electron. Lett., 43, 183-185, 2007.

[30] Y. Tang, “High-speed Optical Transmission System Using Coherent Optical Orthogonal Frequency-Division Multiplexing”, University of Melbourne Australia, 2010.

[31] Y. Tang et al.: “Optimum Design for RF-to-Optical Up-Converter in Coherent Optical OFDM Systems”, IEEE Photonics Technology Letters, vol.19, No.7, April 2007.

[32] Konstantinos Eleftherios Zarganis, Antonis Hatziefremidis, “Performance Analysis of Coherent Optical OFDM Applied to UAV Mobile FSO Systems”, Department of Aircraft.

[33] H. Yang, et al., “Evaluation of Effects of MZM Nonlinearity on QAM and OFDM Signals in RoF Transmitter,”IEEE, pp. 90-93, 2008.

[34] J. C. Cartledge, “Performance of 10 Gb / s Lightwave Systems Based on Lithium Niobate Mach-Zehnder Modulators with Asymmetric Y-Branch Waveguides,” IEEE, vol/issue: 7(9), pp. 1090-1092, 1995.

[35] M.Z. Chowdhury, M.T. Hossan, A. Islam, Y.-M. Jang, “A comparative survey of optical wireless technologies: architectures and applications”, IEEE Access 6 (Jan. 2018) 9819-9840.

[36] M. Saadi, L. Wuttisittikulkij, “Visible light communication-the journey so far”, J. Opt. Commun. 40 (4) (Oct. 2017) 1-7.

[37] M. N. O. Sadiku S.M. Musa, “Free Space Optical Communications: An Overview”, SEET, Pennsylvania State University Erie, PA, 2016.

[38] G.P. Agrawal, “Fiber-Optic Communication Systems,” John Wiley & Sons, Hoboken, N.J, 2010.

[39] M.Z. Chowdhury, M.T. Hossan, A. Islam, Y.-M. Jang, “A comparative survey of optical wireless technologies: architectures and applications”, IEEE Access 6 (Jan. 2018) 9819-9840.

[40] S.U. Rehman, S. Ullah, P.H.J. Chong, S. Yongchareon, D. Komosny, “Visible light communication: a system perspective overview and challenges”, Sensors 19 (5) (2019), pp. 1153:1-22.

[41] M. Uysal, H. Nouri, “Optical wireless communications-an emerging technology”, in: Proc. Of IEEE the 16th Intl. Conf. on Transparent Optical Networks, Graz, 2014, pp. 1-7.

[42] M.A. Khalighi, M. Uysal, “Survey on free space optical communication: a communication theory perspective”, IEEE Commun. Survey Tutorial 16 (4) (Jun. 2014) 2231-2258.

[43] A.H.A. El-Malek, A.M. Salhab, S.A. Zummo, M.S. Alouini, “Effect of RF interference on the security-reliability tradeoff analysis of multiuser mixed RF/FSO relay networks with power allocation”, J. Lightwave Technol. 35 (9) (May 2017) 1490-1505.

[44] B. Smutny, H. Kaempfner, G. Muehlnikel, et al., “5.6 Gbps optical intersatellite communication link”, in: Proc. OfSPIE 7199, Free-Space Laser Communication Technologies XXI, San Jose, 2009, pp. 719906:1-8.

[45] A.W. Azim, “Signal Processing Techniques for Optical Wireless Communication Systems”, Ph.D. dissertation, Universit_e Grenoble Alpes, Grenoble, France, 2018.

[46] J. Kaufmann, “Free space optical communications: an overview of applications and technologies,” in Proceedings of the Boston IEEE Communications Society Meeting, 2011.

[47] M. N. O. Sadiku, S.M. Musa, “Free Space Optical Communications: An Overview”, College of Engineering, Prairie View A&M University, Prairie, 2016.

[48] A. Malik and P. Singh, “Free Space Optics: Current Applications and Future Challenges”, University Institute of Engineering & Technology, Panjab University, Chandigarh, India, 2015.

[49] D. Felice,“A Study of a Nonlinear Schr□odinger Equation for Optical Fibers”, Florentina Studiorum University, arXiv: 1612.00358v1 [math-ph], 1 Dec 2016.

[50] G. Keiser, “Optical Fiber Communications,” McGraw- Hill Education, New York, 2011.

[51] G.P. Agrawal, “Fiber-Optic Communication Systems,” John Wiley & Sons, Hoboken, N.J, 2010.

[52] M. Alnoor, “Green Radio Communication Networks Applying Radio-over-fiber Technology for Wireless Access,” PhD Thesis, Middlesex University, UK, 2011.

[53] G. P. Agrawal, "Nonlinear fibre optics," Academic Press, 1995.

[54] X. Zheng, "Advanced Optical OFDM Transceivers for Optical Access Networks," PhD Thesis, Bangor University, 2011.

[55] Q. Lin and G. P. Agrawal, “Vector theory of cross-phase modulation: Role of nonlinear polarization rotation,” IEEE J. Quantum Electron., vol. 40, no. 7, pp. 958-964, Jul. 2004.

[56] M. Jarajreh, “Coherent Optical OFDM Modem Employing Artificial Neural Networks for Dispersion and nonlinearity Compensation in a Long-Transmission System,” PhD thesis, University of Northumbria, Newcastle, 2012.

[57] V. S. Oleg, “Calculation of Bit Error Rates in Optical Fiber Communications Systems in the Presence of Nonlinear Distortion and Noise”, University of Maryland, 2006.

[58] R. S. Luís and A. V. T. Cartaxo, “Analytical characterization of SPM impact on XPM-induced degradation in dispersion-compensated WDM systems”, J. Lightwave Technol., vol. 23, pp. 1503_1513, 2005.

[59] A. Cartaxo, “Cross-phase modulation in intensity modulation direct detection WDM systems with multiple optical amplifiers and dispersion compensators”, J. Lightwave Technol., vol. 17, pp. 178_190, 1999.

[60] A.W. Azim, “Signal Processing Techniques for Optical Wireless Communication Systems”, Ph.D. dissertation, Universit_e Grenoble Alpes, Grenoble, France, 2018.

[61] J. Kaufmann, “Free space optical communications: an overview of applications and technologies,” in Proceedings of the Boston IEEE Communications Society Meeting, 2011.

[62] M. N. O. Sadiku, S.M. Musa, “Free Space Optical Communications: An Overview”, College of Engineering, Prairie View A&M University, Prairie, 2016.

[63] Ming Zhu, “high-capacity communication systems using advanced optical and wireless technologies”, Georgia Institute of Technology, May, 2015.

[64] G.P. Agrawal, “Fiber-Optic Communication Systems,” John Wiley & Sons, Hoboken, N.J, 2010.

[65] S. Bloom et al.: “Understanding the performance of free-space optics”,Journal of Optical Networking, Vol.2, No.6, June 2003

[66] E. Ciaramella, Y. Arimoto, G. Contestabile, M. Presi, A. D. Errico, V. Guarino, and M. Matsumoto, “1.28 Terabits (32x40 Gbits) WDM Transmission System for Free Space Optical Communications", IEEE Journal on selected Areas in Communications, vol. 27, no. 9, pp. 1639-1645, December 2009.

[67] P. Chen, S. Chang, S. Shuen-Te Ji, H. Lin, H. Tsay, P. Huang, W. Chiang, W. Lin, S. Lee, H. Tsao, “Demonstration of 16 channels 10 Gb/s WDM free space transmission over 2.16 km”, IEEE/LEOS Summer Topical Meetings, pp. 235-236, 2008.

[68] E. Yamada, A. Sano, H. Masuda, T. Kobayashi, E. Yoshida, Y. Miyamoto, Y. Hibino, K. Ishihara, Y. Takatori, K. Okada, K. Hagimoto, T. Yamada, and H. Yamazaki, “Novel no-guardinterval PDM CO-OFDM transmission in 4.1 Tb/s (50 88.8-Gb/s) DWDM link over 800 km SMF including 50-GHz spaced ROADM nodes” Opt. Fiber Commun. Conf., paper PDP8, San Diego, CA, USA, 2008.

[69] Leitgeb E., Bregenzer J., Fasser P., Gebhar M., “Free Space Optics - Extension to Fiber-Networks for the ”Last Mile”. Lasers and Electro-Optics Society”, LEOS, the 15th Annual Meeting of the IEEE, Technische Univ. Graz, Austria, 2002, 459-60.

[70] Bloom, S., Hartley, W. S., “The Last-Mile Solution: Hybrid FSO Radio”, white papers AirFiber, Inc, http://www. Free space optic.com/White Papers/Hybrid FSO.pd f :, 2002, 1-20.

[71] Kim, A., Ju, Y., Kim, Y. S., Nahm, S. M., “Hybrid Fiber Radio Systems for Pico-Cell Communications”, Microwave and Optical Technology Letters 33-5:328-30, 2002.